COOPERATIVE VISIBLE LIGHT POSITIONING SYSTEMS

A THESIS SUBMITTED TO
THE GRADUATE SCHOOL OF ENGINEERING AND SCIENCE
OF BILKENT UNIVERSITY
IN PARTIAL FULFILLMENT OF THE REQUIREMENTS FOR
THE DEGREE OF
MASTER OF SCIENCE
IN
ELECTRICAL AND ELECTRONICS ENGINEERING

By
Osman Erdem
December 2017

COOPERATIVE VISIBLE LIGHT POSITIONING SYSTEMS
By Osman Erdem
December 2017

We certify that we have read this thesis and that in our opinion it is fully adequate, in scope and in quality, as a thesis for the degree of Master of Science.

Sinan Gezici(Advisor)

Süleyman Serdar Kozat

Çağatay Candan

Approved for the Graduate School of Engineering and Science:

Ezhan Karaşan
Director of the Graduate School

ABSTRACT

COOPERATIVE VISIBLE LIGHT POSITIONING SYSTEMS

Osman Erdem
M.S. in Electrical and Electronics Engineering
Advisor: Sinan Gezici
December 2017

Light emitting diode (LED) based visible light positioning (VLP) systems offer an alternative approach to commonly used radio frequency (RF) based positioning systems. In the literature, VLP studies are performed only for noncooperative systems. In this thesis, received signal strength (RSS) based cooperative localization is proposed for visible light systems. The effects of cooperation on the localization accuracy of visible light positioning systems are illustrated based on a Cramér-Rao lower bound expression. The obtained expression is generic for any three-dimensional configuration and covers all possible cooperation scenarios via definitions of connectivity sets. In addition, a low-complexity positioning algorithm is proposed for cooperative location estimation. Numerical results are presented to investigate the significance of cooperation and to evaluate performance of the proposed algorithm in various scenarios.

Keywords: Positioning, visible light, cooperative localization, estimation, received signal strength.

ÖZET

İŞBİRLİKÇİ GÖRÜNÜR IŞIK KONUMLANDIRMA SİSTEMLERİ

Osman Erdem
Elektrik Elektronik Mühendisliği, Yüksek Lisans
Tez Danışmanı: Sinan Gezici
Aralık 2017

Işık saçan diyot (LED) kullanılarak yapılan görünür ışık konumlandırma sistemleri, yaygın olarak kullanılan radyo frekansı bazlı konumlandırma sistemlerine alternatif oluşturmaktadır. Literatürdeki görünür ışık konumlandırma çalışmaları, işbirlikçi olmayan sistemler üzerinde uygulanmaktadır. Bu tezde, görünür ışık sistemleri için alınan sinyal gücü ölçümlerine dayanan işbirlikçi konumlandırma sistemi önerilmektedir. Konumlandırma doğruluğu üzerine işbirliğinin etkisi, Cramer-Rao alt sınırı ifadesi kullanılarak gösterilmektedir. Türetilen ifade, herhangi bir üç boyutlu kurulum için geçerlidir ve bağlantı setleri tanımı vasıtasıyla olası bütün işbirliği senaryolarını kapsamaktadır. Buna ek olarak, işbirlikçi konumlandırma için düşük karmaşıklık içeren bir konumlandırma algoritması önerilmektedir. İşbirliğinin önemini ve önerilen algoritmanın çeşitli senaryolarda performansını değerlendirmek için sayısal örnekler sunulmaktadır.

Anahtar sözcükler: Konumlandırma, görünür ışık, işbirlikçi konumlandırma, kestirim, gelen işaret gücü.

Acknowledgement

First of all, I would like to show my gratitude to my supervisor Prof. Dr. Sinan Gezici for his continuous optimism concerning this work, encouragement and support. The door to his office was always open whenever I ran into a trouble spot or had a question about my research. I could not have imagined having a better advisor.

I would like to thank Assoc. Prof. Süleyman Serdar Kozat and Prof. Çağatay Candan for agreeing to be on my thesis committee.

I must express my gratitude to Musa Furkan Keskin and Furkan Kökdoğan for their valuable contributions to my study.

I would also like to offer my special thanks to Dilan Öztürk who had truly helped me to maintain my motivation. I am thankful to my office colleagues Ertan Kazıklı, İbrahim Kurban Özaslan and Kübra Keskin for their support as well.

I appreciate the financial support of The Scientific and Technological Research Council of Turkey (TÜBİTAK), through BİDEB 2228-A Scholarship Program during my study.

I would like to thank my family, my mother Hayriye, my father Resul and my drummer brother Alper for their support and encouragement in my whole life.

Finally, I would like to express my gratitude to my girlfriend Şeyma Akgül for her love and encouragement. Thank you for supporting me in every way.

Contents

List of Figures

List of Tables

Chapter 1

Introduction

Accurate wireless positioning is crucial for indoor environments in order to facilitate applications such as patient monitoring, inventory tracking, and robotic control [1]–[3]. Although radio frequency (RF) based solutions are commonly employed for wireless indoor positioning [1, 2, 4, 5], light emitting diode (LED) based visible light positioning (VLP) systems have recently emerged as an appealing alternative [6].

Besides localization, visible light systems can also provide illumination and data communication simultaneously. In addition, they do not incur additional installation costs due to the trend of using LEDs for efficient illumination, since LEDs have long lifetime and low power consumption in comparison to conventional light bulbs. Another superior side of LEDs is that they have high modulation capability [7]. Modulating the LEDs on the order of MHz, high-rate data transmission can be provided without human eye perception. With these features, LEDs are expected to replace traditional light bulbs [8], forming a basis for visible light communication (VLC) and VLP in indoor environments.

The visible light system in this thesis consists of LEDs on a ceiling and multiple VLC units. In each VLC unit, there exist LEDs and photo-detectors (PDs). The PDs measure the optical power coming from the LEDs in the field of view,

and communication and positioning are performed based on those power measurements. While the LEDs on the ceiling are utilized for noncooperative positioning, measured power levels due to the LEDs on the VLC units are employed for cooperation, as depicted in Fig. 1.1. In this thesis, cooperative positioning is proposed for VLP systems for improving localization accuracy.

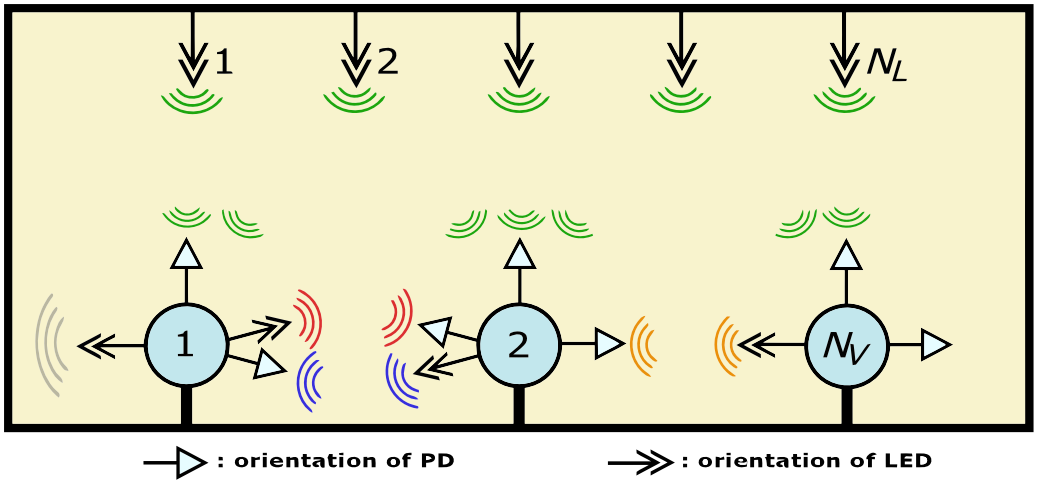

Figure 1.1: Cooperative VLP system, where the arrows denote LEDs and triangles represent PDs.

1.1 Related Work

Positioning problem is commonly considered as noncooperative, where only the measurements between target and reference nodes are used for position estimation. When there exist a limited number of reference nodes, the positioning accuracy can decrease considerably in noncooperative systems. To overcome this issue, a cooperative (or collaborative) approach can be employed. The main idea behind cooperation is to utilize measurements among target nodes (which are to be located) in addition to those between target nodes and reference nodes (which have known locations). In this way, localization accuracy can be enhanced based

on the relative location information obtained from the measurements among target nodes [9].

In the literature, cooperation techniques are intensely studied for RF based positioning systems (see [9] and references therein). There exist numerous algorithms for various cooperation scenarios and some recent works focus on fundamental limits for cooperative positioning systems [10]–[18]. For example, in [11], network experiments are conducted using ultra-wideband (UWB) signals, and comparisons between cooperative and noncooperative positioning systems are performed to reveal the benefits of cooperative positioning under a common setting. The study in [17] presents an overview of cooperative positioning algorithms from the viewpoint of estimation theory and factor graphs. It proposes a distributed cooperative positioning algorithm and compares its performance against other conventional noncooperative and cooperative positioning techniques. In [16], a cooperative wireless sensor network in the presence of unknown turn-around times is considered. Measuring two-way time-of-arrival (TW-TOA) and time-difference-of-arrival (TDOA) using two different reference sensors, multiple target node positioning is addressed. The work in [13] uses hybrid WiMAX/Wi-Fi simulations for an outdoor environment, using combination of TDOA and received signal strength (RSS) measurements.

Although cooperation techniques have been considered for RF based positioning systems, there exist no studies in the literature that perform visible light positioning in the presence of cooperation.

1.2 Thesis Overview

In this thesis, a cooperative VLP system is proposed and a theoretical analysis is provided by deriving a generic Cramér-Rao lower bound (CRLB) expression. The provided expression is valid for any three-dimensional configuration and covers all possible cooperation scenarios via definitions of connectivity sets. Although CRLB expressions are obtained for VLP systems in [19]–[25], all of them are for

noncooperative systems and consider the presence of a single VLP receiver. In particular, [19]–[23] focus on distance estimation between an LED transmitter and a VLP receiver while [24] and [25] derive CRLBs for RSS based position estimation for a single VLP receiver.

In this thesis, cooperative positioning is proposed for visible light systems, in which there exist multiple LED transmitters with known locations and multiple VLC units to be located. Each VLC unit is modeled to contain multiple LEDs and multiple PDs so that it can communicate with both the LED transmitters at known locations and the other VLC units. By defining a connectivity set for each PD in the VLC units, all possible cooperation scenarios are taken into account. The CRLB expression is derived for estimating the locations of the VLC receivers, and based on the proposed expression, the effects of cooperation are quantified. The provided CRLB expression is generic for any configuration and covers the noncooperative scenario as a special case. Numerical results are presented to investigate the significance of cooperation in various conditions.

The main contributions of this thesis can be summarized as the proposal of a cooperative VLP system for the first time in the literature, and the derivation of a generic CRLB expression for cooperative VLP systems. In addition, a sequential location estimation algorithm is proposed, which has low computational complexity. (Some of the results in this thesis are presented in [26].)

The rest of the thesis is organized as follows: The system model is described and the CRLB expression is derived in Chapter 2. In Chapter 3, a sequential location estimation algorithm is proposed for cooperative VLP systems. Numerical results and simulations are presented in Chapter 4 and Chapter 5, respectively. Concluding remarks are made and future research directions are discussed in Chapter 6.

Chapter 2

System Model and Theoretical Analysis

The proposed cooperative VLP system consists of N_L LED transmitters and N_V VLC units, as illustrated in Fig. 2.1. The location of the jth LED transmitter is denoted by $\mathbf{y}_j$ and its orientation vector is given by $\widetilde{\mathbf{n}}_{T,j}$ for $j \in \{1, \ldots, N_L\}$. The locations and the orientations of the LED transmitters are assumed to be known, which is a reasonable assumption for practical systems [24, 27]. In the proposed system, each VLC unit not only gathers signals from the LED transmitters but also communicates with other VLC units in the system for cooperation purposes. To that aim, VLC units are equipped with both LEDs and PDs; namely, there exist L_i LEDs and K_i PDs at the ith VLC unit for $i \in \{1, \ldots, N_V\}$. The unknown location of the ith VLC unit is denoted by $\mathbf{x}_i$, where $i \in \{1, \ldots, N_V\}$. For the jth PD at the ith VLC unit, the location is given by $\mathbf{x}_i + \mathbf{a}_{i,j}$ and the orientation vector is denoted by $\mathbf{n}_{R,j}^{(i)}$, where $j \in \{1, \ldots, K_i\}$. Similarly, for the jth LED at the ith VLC unit, the location is given by $\mathbf{x}_i + \mathbf{b}_{i,j}$ and the orientation vector is represented by $\mathbf{n}_{T,j}^{(i)}$, where $j \in \{1, \ldots, L_i\}$. The displacement vectors, $\mathbf{a}_{i,j}$'s and $\mathbf{b}_{i,j}$'s, are known design parameters for the VLC units. Also, the orientation vectors for the LEDs and PDs at the VLC units are assumed to be known since they can be determined by the VLC unit design and by auxiliary sensors (e.g., gyroscope). To distinguish the LED transmitters at known locations from the

LEDs at the VLC units, the former are called as the LEDs *on the ceiling* (as in Fig. 2.1) in the remainder of the thesis.

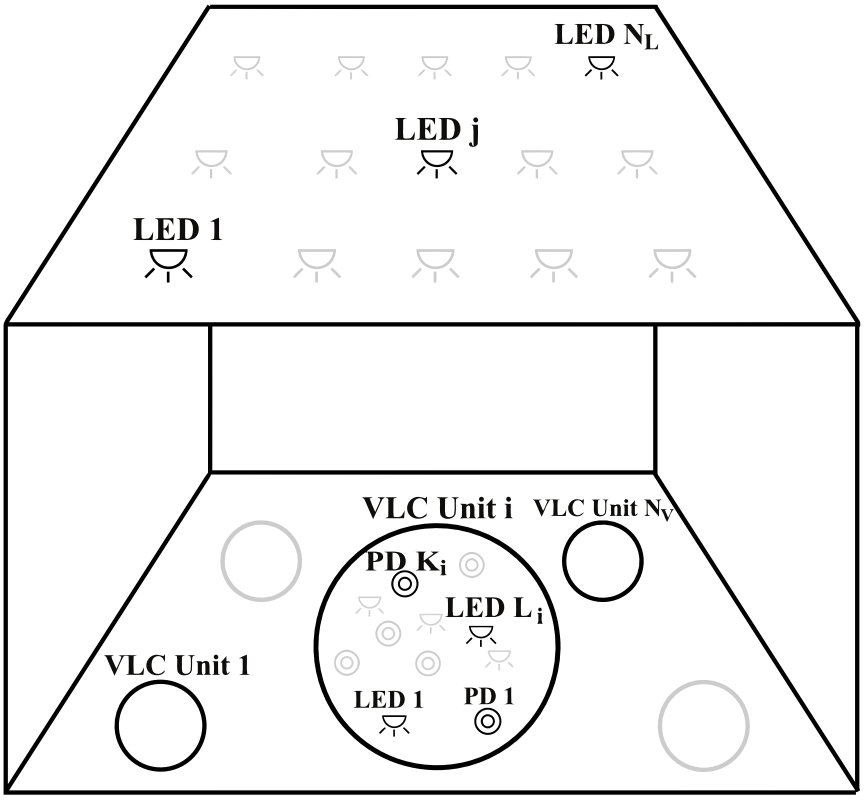

Figure 2.1: Cooperative VLP system.

At a given time, each PD can communicate with a subset of all the LEDs in the system. Therefore, the following connectivity sets are defined to specify the

connections between the LEDs and the PDs:

$$\widetilde{S}_k^{(j)} = \big\{ l \in \{1,\ldots,N_L\} \mid l\text{th LED on ceiling is connected to } k\text{th PD of } j\text{th VLC unit} \big\} \tag{2.1}$$

$$S_k^{(i,j)} = \big\{ l \in \{1,\ldots,L_i\} \mid l\text{th LED of } i\text{th VLC unit is connected to } k\text{th PD of } j\text{th VLC unit} \big\}. \tag{2.2}$$

Namely, $\widetilde{S}_k^{(j)}$ represents the set of LEDs on the ceiling that are connected to the kth PD at the jth VLC unit. Similarly, $S_k^{(i,j)}$ is the set of LEDs at the ith VLC unit that are connected to the kth PD at the jth VLC unit.

The aim is to estimate the unknown locations, $\mathbf{x}_1,\ldots,\mathbf{x}_{N_V}$, of the VLC units based on power measurements at the PDs. Let $\widetilde{P}_{l,k}^{(j)}$ represent the power measurement at the kth PD of the jth VLC unit due to the transmission from the lth LED on the ceiling. Similarly, let $P_{l,k}^{(i,j)}$ denote the power measurements at the kth PD of the jth VLC unit due to the lth LED at the ith VLC unit. Based on the Lambertian formula [19, 28], $\widetilde{P}_{l,k}^{(j)}$ and $P_{l,k}^{(i,j)}$ can be expressed as follows:

$$\widetilde{P}_{l,k}^{(j)} = \frac{\widetilde{m}_l + 1}{2\pi} \widetilde{P}_{T,l} \cos^{\widetilde{m}_l}(\widetilde{\phi}_{l,k}^{(j)}) \cos(\widetilde{\theta}_{l,k}^{(j)}) \frac{A_k^{(j)}}{\left(\widetilde{d}_{l,k}^{(j)}\right)^2} + \widetilde{\eta}_{l,k}^{(j)} \tag{2.3}$$

for $j \in \{1,\ldots,N_V\}$, $k \in \{1,\ldots,K_j\}$, and $l \in \widetilde{S}_k^{(j)}$, and

$$P_{l,k}^{(i,j)} = \frac{m_l^{(i)} + 1}{2\pi} P_{T,l}^{(i)} \cos^{m_l^{(i)}}(\phi_{l,k}^{(i,j)}) \cos(\theta_{l,k}^{(i,j)}) \frac{A_k^{(j)}}{\left(d_{l,k}^{(i,j)}\right)^2} + \eta_{l,k}^{(i,j)} \tag{2.4}$$

for $j \in \{1,\ldots,N_V\}$, $k \in \{1,\ldots,K_j\}$, $i \in \{1,\ldots,N_V\} \setminus j$ and $l \in S_k^{(i,j)}$, where the distances $\widetilde{d}_{l,k}^{(j)}$ and $d_{l,k}^{(i,j)}$ are given by

$$\widetilde{d}_{l,k}^{(j)} = \left\| \widetilde{\mathbf{d}}_{l,k}^{(j)} \right\| \text{ with } \widetilde{\mathbf{d}}_{l,k}^{(j)} \triangleq \mathbf{x}_j + \mathbf{a}_{j,k} - \mathbf{y}_l \tag{2.5}$$

$$d_{l,k}^{(i,j)} = \left\| \mathbf{d}_{l,k}^{(i,j)} \right\| \text{ with } \mathbf{d}_{l,k}^{(i,j)} \triangleq \mathbf{x}_j + \mathbf{a}_{j,k} - \mathbf{x}_i - \mathbf{b}_{i,l}\,. \tag{2.6}$$

In (2.3) and (2.4), $\widetilde{m}_l$ ($m_l^{(i)}$) is the Lambertian order for the lth LED on the ceiling (at the ith VLC unit), $A_k^{(j)}$ is the area of the kth PD at the jth VLC unit, $\widetilde{P}_{T,l}$ ($P_{T,l}^{(i)}$) is the transmit power of the lth LED on the ceiling (at the ith VLC unit), $\widetilde{\phi}_{l,k}^{(j)}$ ($\phi_{l,k}^{(i,j)}$) is the irradiation angle at the lth LED on the ceiling (at

the ith VLC unit) with respect to the kth PD at the jth VLC unit, and $\widetilde{\theta}_{l,k}^{(j)}$ ($\theta_{l,k}^{(i,j)}$) is the incidence angle for the kth PD at the jth VLC unit related to the lth LED on the ceiling (at the ith VLC unit). In addition, the noise components, $\widetilde{\eta}_{l,k}^{(j)}$ and $\eta_{l,k}^{(i,j)}$, are modeled by zero-mean Gaussian random variables each with a variance of $\sigma_{j,k}^2$. Considering the use of a certain multiplexing scheme (e.g., time division multiplexing among the LEDs at the same VLC unit and on the ceiling, and frequency division multiplexing among the LEDs at different VLC units or on the ceiling), $\widetilde{\eta}_{l,k}^{(j)}$ and $\eta_{l,k}^{(i,j)}$ are assumed to be independent for all different (j,k) pairs and for all l and i.

From (2.5) and (2.6), the power measurements in (2.3) and (2.4) can also be expressed as

$$\widetilde{P}_{l,k}^{(j)} = \widetilde{\alpha}_{l,k}^{(j)}(\mathbf{x}_j) + \widetilde{\eta}_{l,k}^{(j)} \tag{2.7}$$

$$P_{l,k}^{(i,j)} = \alpha_{l,k}^{(i,j)}(\mathbf{x}_i, \mathbf{x}_j) + \eta_{l,k}^{(i,j)} \tag{2.8}$$

where

$$\widetilde{\alpha}_{l,k}^{(j)}(\mathbf{x}_j) \triangleq -\frac{\widetilde{m}_l + 1}{2\pi} \widetilde{P}_{T,l} A_k^{(j)} \frac{\left((\widetilde{\mathbf{d}}_{l,k}^{(j)})^T \widetilde{\mathbf{n}}_{T,l}\right)^{\widetilde{m}_l} (\widetilde{\mathbf{d}}_{l,k}^{(j)})^T \mathbf{n}_{R,k}^{(j)}}{\left\| \widetilde{\mathbf{d}}_{l,k}^{(j)} \right\|^{\widetilde{m}_l + 3}} \tag{2.9}$$

$$\alpha_{l,k}^{(i,j)}(\mathbf{x}_i, \mathbf{x}_j) \triangleq -\frac{m_l^{(i)} + 1}{2\pi} P_{T,l}^{(i)} A_k^{(j)} \frac{\left((\mathbf{d}_{l,k}^{(i,j)})^T \mathbf{n}_{T,l}^{(i)}\right)^{m_l^{(i)}} (\mathbf{d}_{l,k}^{(i,j)})^T \mathbf{n}_{R,k}^{(j)}}{\left\| \mathbf{d}_{l,k}^{(i,j)} \right\|^{m_l^{(i)} + 3}} . \tag{2.10}$$

Let $\mathbf{x} \triangleq \left[\mathbf{x}_1^T \dots \mathbf{x}_{N_V}^T\right]^T$ denote the vector of unknown parameters (which has a size of $3N_V \times 1$) and let $\mathbf{P}$ represent a vector consisting of all the measurements in (2.7) and (2.8). The elements of $\mathbf{P}$ can be expressed as follows: $\left\{ \left\{ \left\{ \widetilde{P}_{l,k}^{(j)} \right\}_{l \in \widetilde{S}_k^{(j)}} \right\}_{k \in \{1,\dots,K_j\}} \right\}_{j \in \{1,\dots,N_V\}}$, $\left\{ \left\{ \left\{ \left\{ P_{l,k}^{(i,j)} \right\}_{l \in S_k^{(i,j)}} \right\}_{i \in \{1,\dots,N_V\} \setminus \{j\}} \right\}_{k \in \{1,\dots,K_j\}} \right\}_{j \in \{1,\dots,N_V\}}$. Then, the conditional probability density function (PDF) of $\mathbf{P}$ given $\mathbf{x}$, i.e., the likelihood function, can be stated as

$$f(\mathbf{P} \,|\, \mathbf{x}) = \prod_{j=1}^{N_V} \prod_{k=1}^{K_j} \left(\prod_{l \in \widetilde{S}_k^{(j)}} f(\widetilde{P}_{l,k}^{(j)} | \mathbf{x}) \times \prod_{i \in \{1,\dots,N_V\} \setminus \{j\}} \prod_{l \in S_k^{(i,j)}} f(P_{l,k}^{(i,j)} | \mathbf{x}) \right) \tag{2.11}$$

where $f(\widetilde{P}_{l,k}^{(j)}|\mathbf{x})$ and $f(P_{l,k}^{(i,j)}|\mathbf{x})$ are the marginal conditional PDFs of $\widetilde{P}_{l,k}^{(j)}$ and $P_{l,k}^{(i,j)}$, respectively. Since $\widetilde{P}_{l,k}^{(j)}|\mathbf{x}$ and $P_{l,k}^{(i,j)}|\mathbf{x}$ are Gaussian distributed with means of $\widetilde{\alpha}_{l,k}^{(j)}(\mathbf{x}_j)$ and $\alpha_{l,k}^{(i,j)}(\mathbf{x}_i,\mathbf{x}_j)$, respectively, and a variance of $\sigma_{j,k}^2$ each (see (2.7) and (2.8)), (2.11) can be specified as

$$f(\mathbf{P}\,|\,\mathbf{x}) = \prod_{j=1}^{N_V}\prod_{k=1}^{K_j}\left(\frac{e^{-\frac{1}{2\sigma_{j,k}^2}\sum_{l\in\widetilde{S}_k^{(j)}}\left(\widetilde{P}_{l,k}^{(j)}-\widetilde{\alpha}_{l,k}^{(j)}(\mathbf{x}_j)\right)^2}}{(\sqrt{2\pi}\sigma_{j,k})^{|\widetilde{S}_k^{(j)}|}}\right.$$
$$\left.\times\prod_{i\in\{1,\ldots,N_V\}\setminus\{j\}}\frac{e^{-\frac{1}{2\sigma_{j,k}^2}\sum_{l\in S_k^{(i,j)}}\left(P_{l,k}^{(i,j)}-\alpha_{l,k}^{(i,j)}(\mathbf{x}_i,\mathbf{x}_j)\right)^2}}{(\sqrt{2\pi}\sigma_{j,k})^{|S_k^{(i,j)}|}}\right) \tag{2.12}$$

where $|\widetilde{S}_k^{(j)}|$ and $|S_k^{(i,j)}|$ represent the number of elements in sets $\widetilde{S}_k^{(j)}$ and $S_k^{(i,j)}$, respectively. After some manipulation, (2.12) can be expressed as

$$f(\mathbf{P}\,|\,\mathbf{x}) = \left(\prod_{j=1}^{N_V}\prod_{k=1}^{K_j}\frac{1}{(\sqrt{2\pi}\,\sigma_{j,k})^{N_{tot}^{(j,k)}}}\right)e^{-\sum_{j=1}^{N_V}\sum_{k=1}^{K_j}\frac{h_{j,k}(\mathbf{x})}{2\sigma_{j,k}^2}} \tag{2.13}$$

where $N_{tot}^{(j,k)}$ represents the total number of LEDs that can communicate with the kth PD at the jth VLC unit; that is,

$$N_{tot}^{(j,k)} \triangleq |\widetilde{S}_k^{(j)}| + \sum_{i=1,i\neq j}^{N_V}|S_k^{(i,j)}| \tag{2.14}$$

and $h_{j,k}(\mathbf{x})$ is defined as

$$h_{j,k}(\mathbf{x}) \triangleq \sum_{l\in\widetilde{S}_k^{(j)}}\left(\widetilde{P}_{l,k}^{(j)}-\widetilde{\alpha}_{l,k}^{(j)}(\mathbf{x}_j)\right)^2 \;+\sum_{i=1,i\neq j}^{N_V}\sum_{l\in S_k^{(i,j)}}\left(P_{l,k}^{(i,j)}-\alpha_{l,k}^{(i,j)}(\mathbf{x}_i,\mathbf{x}_j)\right)^2. \tag{2.15}$$

From (2.13), the maximum likelihood estimator (MLE) is obtained as

$$\hat{\mathbf{x}}_{\mathrm{ML}} = \arg\min_{\mathbf{x}}\sum_{j=1}^{N_V}\sum_{k=1}^{K_j}\frac{h_{j,k}(\mathbf{x})}{\sigma_{j,k}^2} \tag{2.16}$$

and the Fisher information matrix (FIM) [29] is given by

$$[\mathbf{J}]_{t_1,t_2} = \mathbb{E}\left\{\frac{\partial\log f(\mathbf{P}\,|\,\mathbf{x})}{\partial x_{t_1}}\frac{\partial\log f(\mathbf{P}\,|\,\mathbf{x})}{\partial x_{t_2}}\right\} \tag{2.17}$$

where x_{t_1} (x_{t_2}) represents element t_1 (t_2) of vector $\mathbf{x}$ with $t_1, t_2 \in \{1, 2, \ldots, 3N_V\}$. Then, the CRLB is stated as

$$\text{CRLB} = \text{trace}(\mathbf{J}^{-1}) \leq \mathbb{E}\{\|\hat{\mathbf{x}} - \mathbf{x}\|^2\} \tag{2.18}$$

where $\hat{\mathbf{x}}$ represents an unbiased estimator of $\mathbf{x}$. From (2.13) and (2.15), the elements of the FIM in (2.17) can be calculated after some manipulation as

$$\begin{aligned}[\mathbf{J}]_{t_1,t_2} = \sum_{j=1}^{N_V}\sum_{k=1}^{K_j}\frac{1}{\sigma_{j,k}^2}\Bigg(&\sum_{l\in\widetilde{S}_k^{(j)}}\frac{\partial\widetilde{\alpha}_{l,k}^{(j)}(\mathbf{x}_j)}{\partial x_{t_1}}\frac{\partial\widetilde{\alpha}_{l,k}^{(j)}(\mathbf{x}_j)}{\partial x_{t_2}} \\ &+\sum_{i=1,i\neq j}^{N_V}\sum_{l\in S_k^{(i,j)}}\frac{\partial\alpha_{l,k}^{(i,j)}(\mathbf{x}_i,\mathbf{x}_j)}{\partial x_{t_1}}\frac{\partial\alpha_{l,k}^{(i,j)}(\mathbf{x}_i,\mathbf{x}_j)}{\partial x_{t_2}}\Bigg).\end{aligned} \tag{2.19}$$

In addition, from (2.5), (2.6), (2.9), and (2.10), the partial derivatives in (2.19) are obtained as follows:

$$\begin{aligned}\frac{\partial\widetilde{\alpha}_{l,k}^{(j)}(\mathbf{x}_j)}{\partial x_t} &= -\frac{(\widetilde{m}_l+1)\widetilde{P}_{T,l}A_k^{(j)}\big((\widetilde{\mathbf{d}}_{l,k}^{(j)})^T\widetilde{\mathbf{n}}_{T,l}\big)^{\widetilde{m}_l}}{2\pi\left\|\widetilde{\mathbf{d}}_{l,k}^{(j)}\right\|^{\widetilde{m}_l+3}} \\ &\times\Big(\widetilde{m}_l\widetilde{n}_{T,l}(t-3j+3)(\widetilde{\mathbf{d}}_{l,k}^{(j)})^T\mathbf{n}_{R,k}^{(j)}\big((\widetilde{\mathbf{d}}_{l,k}^{(j)})^T\widetilde{\mathbf{n}}_{T,l}\big)^{-1}+n_{R,k}^{(j)}(t-3j+3) \\ &\quad-(\widetilde{m}_l+3)\widetilde{d}_{l,k}^{(j)}(t-3j+3)(\widetilde{\mathbf{d}}_{l,k}^{(j)})^T\mathbf{n}_{R,k}^{(j)}\left\|\widetilde{\mathbf{d}}_{l,k}^{(j)}\right\|^{-2}\Big)\end{aligned} \tag{2.20}$$

for $t \in \{3j-2, 3j-1, 3j\}$ and $\partial\widetilde{\alpha}_{l,k}^{(j)}(\mathbf{x}_j)/\partial x_t = 0$ otherwise, where $\widetilde{n}_{T,l}(t-3j+3)$, $n_{R,k}^{(j)}(t-3j+3)$, and $\widetilde{d}_{l,k}^{(j)}(t-3j+3)$ represent the $(t-3j+3)$th elements of $\widetilde{\mathbf{n}}_{T,l}$, $\mathbf{n}_{R,k}^{(j)}$, and $\widetilde{\mathbf{d}}_{l,k}^{(j)}$, respectively. Similarly,

$$\begin{aligned}\frac{\partial\alpha_{l,k}^{(i,j)}(\mathbf{x}_i,\mathbf{x}_j)}{\partial x_t} &= -\frac{(m_l^{(i)}+1)P_{T,l}^{(i)}A_k^{(j)}\big((\mathbf{d}_{l,k}^{(i,j)})^T\mathbf{n}_{T,l}^{(i)}\big)^{m_l^{(i)}}}{2\pi\left\|\mathbf{d}_{l,k}^{(i,j)}\right\|^{m_l^{(i)}+3}} \\ &\times\Big(m_l^{(i)}n_{T,l}^{(i)}(t-3j+3)(\mathbf{d}_{l,k}^{(i,j)})^T\mathbf{n}_{R,k}^{(j)}\big((\mathbf{d}_{l,k}^{(i,j)})^T\mathbf{n}_{T,l}^{(i)}\big)^{-1}+n_{R,k}^{(j)}(t-3j+3) \\ &\quad-(m_l^{(i)}+3)d_{l,k}^{(i,j)}(t-3j+3)(\mathbf{d}_{l,k}^{(i,j)})^T\mathbf{n}_{R,k}^{(j)}\left\|\mathbf{d}_{l,k}^{(i,j)}\right\|^{-2}\Big)\end{aligned} \tag{2.21}$$

for $t \in \{3j-2, 3j-1, 3j\}$, $\partial\alpha_{l,k}^{(i,j)}(\mathbf{x}_i,\mathbf{x}_j)/\partial x_t$ is equal to the negative of (2.21) with $(t-3j+3)$'s being replaced by $(t-3i+3)$'s for $t \in \{3i-2, 3i-1, 3i\}$, and $\partial\alpha_{l,k}^{(i,j)}(\mathbf{x}_i,\mathbf{x}_j)/\partial x_t = 0$ otherwise. In (2.21), $n_{T,l}^{(i)}(t-3j+3)$ and $d_{l,k}^{(i,j)}(t-3j+3)$ denote the $(t-3j+3)$th elements of $\mathbf{n}_{T,l}^{(i)}$ and $\mathbf{d}_{l,k}^{(i,j)}$, respectively.

Based on (2.18)–(2.21), the CRLB for location estimation can be obtained for cooperative VLP systems. The obtained CRLB expression is generic for any three-dimensional configuration and covers all possible cooperation scenarios via the definitions of the connectivity sets (see (2.1) and (2.2)). To the best of authors' knowledge, no such CRLB expressions have been available in the literature for cooperative VLP systems.

Remark 1: From (2.19), it is noted that the first summation term in the parentheses is related to the information from the LED transmitters on the ceiling whereas the remaining terms are due to the cooperation among the VLC units. In the noncooperative case, the elements of the FIM are given by the expression in the first line of (2.19).

Via (2.18)–(2.21), the effects of cooperation on the accuracy of VLP systems can be quantified, as investigated in Chapter 4.

Chapter 3

Sequential Position Estimation Algorithm

The CRLB expression in (2.18) and (2.19) provides a theoretical limit for positioning accuracy of cooperative VLP systems. To compare it against the performance of a practical estimator, the MLE is obtained as in (2.16). Although the MLE can achieve the CRLB asymptotically, it has high computational complexity. In particular, the problem in (2.16) requires a search over an $3N_V$ dimensional space. Therefore, we propose a low-complexity positioning algorithm in this chapter. The proposed algorithm estimates the positions of VLC units sequentially. Initially, the position of the VLC unit with the maximum total received power from the LEDs on the ceiling is estimated. (In other words, no cooperation is considered in the first step.). Then, this VLC unit is used as a reference node for the second VLC unit (which is chosen according to a certain criterion, as discussed later), and the position of the second VLC unit is estimated based on the power measurements from both the LEDs on the ceiling and the LEDs on the first VLC unit. In this manner, the algorithm continues sequentially until all the VLC units are located.

To formulate the proposed sequential estimator, let $v \in \{1, ..., N_V\}$ denote the sequential estimation step and function g relate parameter v to the index of the

VLC unit whose location is estimated in the vth step. Then, for step v, the following estimator is employed for VLC unit $g(v)$:

$$\hat{\mathbf{x}}_{g(v)} = \arg\min_{\mathbf{x}_{g(v)}} \sum_{k=1}^{K_{g(v)}} \frac{h_{g(v),k}(\mathbf{x}_{g(v)})}{\sigma^2_{g(v),k}} \tag{3.1}$$

where $\hat{\mathbf{x}}_{g(v)}$ is the position estimate of the VLC unit with index $g(v)$ and $\sigma^2_{g(v),k}$ represents the noise variance for the kth PD of VLC unit $g(v)$. In addition, $h_{j,k}(\mathbf{x})$ is given as follows:

$$\begin{aligned} h_{g(v),k}(\mathbf{x}_{g(v)}) \triangleq & \sum_{l \in \widetilde{S}_k^{(g(v))}} \left(\widetilde{P}_{l,k}^{(g(v))} - \widetilde{\alpha}_{l,k}^{(g(v))}(\mathbf{x}_{g(v)})\right)^2 \\ & + \sum_{i \in C_v, i \neq g(v)} \sum_{l \in S_k^{(i,g(v))}} \left(P_{l,k}^{(i,g(v))} - \alpha_{l,k}^{(i,g(v))}(\mathbf{x}_i, \mathbf{x}_{g(v)})\right)^2. \end{aligned} \tag{3.2}$$

where $\widetilde{\alpha}_{l,k}^{(g(v))}$ and $\alpha_{l,k}^{(i,g(v))}$ can be obtained via (2.9) and (2.10) by substituting $j = g(v)$, and C_v is the set of index values corresponding to VLC units whose locations are already estimated until step v, which can be defined as:

$$C_v \triangleq \begin{cases} \emptyset, & \text{if } v = 1 \\ \{g(1), g(2), ..., g(v-1)\}, & \text{if } v > 1 \end{cases} \tag{3.3}$$

The pseudo-code of the proposed algorithm is shown in Algorithm 1. For investigating the effects of choosing different initial VLC units for localization, the first estimation index may be determined in a different manner from the one in the algorithm, which is elaborated in Chapter 5.

Since the power measurements from the other VLC units are not utilized in the first step of the algorithm, the first estimator in the algorithm is as in the non-cooperative case. However, in the upcoming steps of the algorithm, the effects of cooperation can be observed more effectively.

Algorithm 1 Total measured power based sequential positioning algorithm for cooperative VLP systems.

Input:

- Positions of LED transmitters on the ceiling: $\mathbf{y}_1,\ \mathbf{y}_2,\ \ldots,\ \mathbf{y}_{N_L}$
- Orientation vectors of all LEDs and PDs in the system:

$$\left\{\widetilde{\mathbf{n}}_{T,l}\right\}_{l\in\{1,\ldots,N_L\}}$$
$$\left\{\left\{\mathbf{n}_{T,l}^{(j)}\right\}_{l\in\{1,\ldots,L_j\}}\right\}_{j\in\{1,\ldots,N_V\}}$$
$$\left\{\left\{\mathbf{n}_{R,k}^{(j)}\right\}_{k\in\{1,\ldots,K_j\}}\right\}_{j\in\{1,\ldots,N_V\}}$$

- Power measurements of PDs:

$$\left\{\left\{\left\{\widetilde{P}_{l,k}^{(j)}\right\}_{l\in\widetilde{S}_k^{(j)}}\right\}_{k\in\{1,\ldots,K_j\}}\right\}_{j\in\{1,\ldots,N_V\}}$$
$$\left\{\left\{\left\{\left\{P_{l,k}^{(i,j)}\right\}_{l\in S_k^{(i,j)}}\right\}_{i\in\{1,\ldots,N_V\}\setminus\{j\}}\right\}_{k\in\{1,\ldots,K_j\}}\right\}_{j\in\{1,\ldots,N_V\}}$$

- Constant system parameters: m, FOV of PDs, PD area

Output:

- Estimated positions of VLC units.

for $v \in \{1,\ldots,N_V\}$ **do**
  Update C_v according to (3.3).
  for each VLC unit i, where $i \notin C_v$ **do**
    Sum the powers measured by all PDs in VLC unit i, coming from LEDs on the ceiling and on the other VLC units in C_v.
  end for
  Find index i_{max}, for which PDs at VLC unit i_{max} receive the highest total power and set $g(v) = i_{max}$, where $i_{max} \in \{1,\ldots,N_V\} \setminus C_v$.
  Estimate the position of VLC unit $g(v)$, as $\hat{\mathbf{x}}_{g(v)}$ based on the estimator given in (3.1)
end for
return estimated positions $\hat{\mathbf{x}}_{g(v)}$ for $v \in \{1,\ldots,N_V\}$.

Chapter 4

Numerical Examples for Theoretical Bounds

In this chapter, theoretical bounds on cooperative localization are investigated to illustrate the effects of cooperation on localization accuracy. VLP system parameters are determined in a similar way to the studies in [19] and [21]. The area of each PD is set to $1\,\mathrm{cm}^2$ and the Lambertian order of all the LEDs is selected as $m = 1$. In addition, the noise variances are calculated using [30, Eq. 6] and [31, Eq. 20]. The parameters for noise variance calculation are set to be the same as those used in [30] (see Table I in [30]). Comparisons are performed for different numbers of cooperating PDs and LEDs, and various numbers of VLC units. In the examples, the PD on top of each VLC unit, which is used for noncooperative positioning, points upwards for all VLC units; i.e., $\mathbf{n}_{R,i}^{(1)} = [0\ 0\ 1]^T$, $i \in \{1, \ldots, N_V\}$. In this chapter, the *number of cooperating elements* is defined as the number of LEDs and PDs that are used for cooperation in each VLC unit, and it is taken to be the same for all VLC units. The cooperating elements are pointing outwards from each VLC unit and the angle between consecutive PDs and LEDs are the same for any number of cooperating elements. For example, in Fig. 4.1, the number of cooperating elements is 3, there exist 3 LEDs and 4 PDs (3 for cooperation) at each VLC unit, and the angle between consecutive PDs and LEDs becomes 60°.

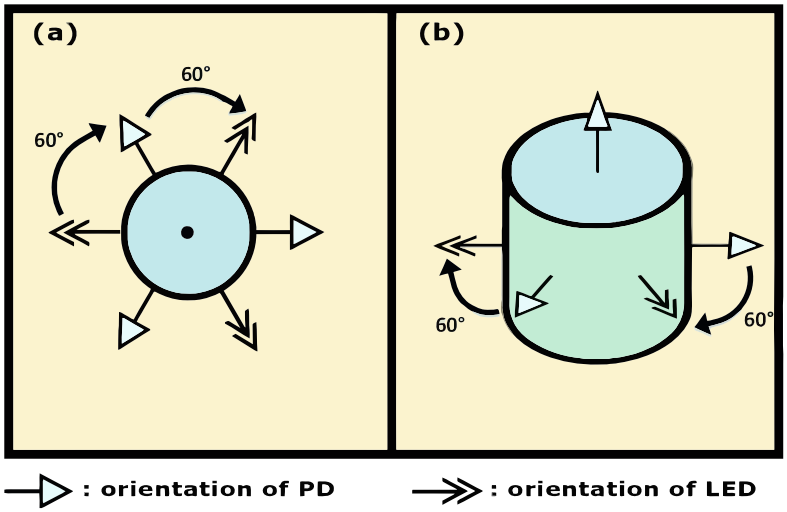

Figure 4.1: VLC unit with 3 cooperating LEDs and PDs. (a) Top view. (b) Isometric view.

4.1 Scenario 1: 2 VLC Unit, 1 Cooperating Element

The VLP system considered in the first example is illustrated in Fig. 4.2. A room of size 5m×5m×4m is considered, where there exist $N_L = 4$ LED transmitters on the ceiling which are located at $\mathbf{y}_1 = [1\ 1\ 4]^T$m., $\mathbf{y}_2 = [1\ 4\ 4]^T$m., $\mathbf{y}_3 = [4\ 1\ 4]^T$m., and $\mathbf{y}_4 = [4\ 4\ 4]^T$m. The orientations of the LEDs on the ceiling are adjusted so that each LED is directed towards the center of the room with an offset angle of 10° with respect to the normal vector of the ceiling. In addition to the LEDs on the ceiling, there exist $N_V = 2$ VLC units whose locations are given by $\mathbf{x}_1 = [2.5\ 2.5\ 1]^T$m. and $\mathbf{x}_2 = [1.5\ 2.5\ 0.5]^T$m. Each VLC unit consists of two PDs and one LED, with offsets with respect to the center of the VLC unit being set to $\mathbf{a}_{j,1} = [0\ -0.1\ 0]^T$m., $\mathbf{a}_{j,2} = [0\ 0.1\ 0]^T$m., and $\mathbf{b}_{j,1} = [0.1\ 0\ 0]^T$m. for $j = 1, 2$. The orientation vectors of the PDs and the LEDs on the VLC units are obtained as the normalized versions (the orientation vectors are unit-norm) of the following vectors: $\mathbf{n}_{R,1}^{(1)} = [0.1\ 0\ 1]^T$, $\mathbf{n}_{R,1}^{(2)} = [0.6\ -0.3\ 1]^T$, $\mathbf{n}_{R,2}^{(1)} = [-0.9\ 0.2\ -0.3]^T$, $\mathbf{n}_{R,2}^{(2)} = [0.2\ -0.1\ 0.1]^T$, $\mathbf{n}_{T,1}^{(1)} = [-0.2\ 0.3\ 0.1]^T$, and

$\mathbf{n}_{T,1}^{(2)} = [0.6\ 0.1\ 0.1]^T$. Furthermore, the connectivity sets are defined as $S_1^{(i,j)} = \emptyset$, $S_2^{(i,j)} = \{1\}$ for $i, j \in \{1, 2\}, i \neq j$ in the cooperative case and $\widetilde{S}_1^{(j)} = \{1, 2, 3, 4\}$, $\widetilde{S}_2^{(j)} = \emptyset$ for $j \in \{1, 2\}$ in the noncooperative case.

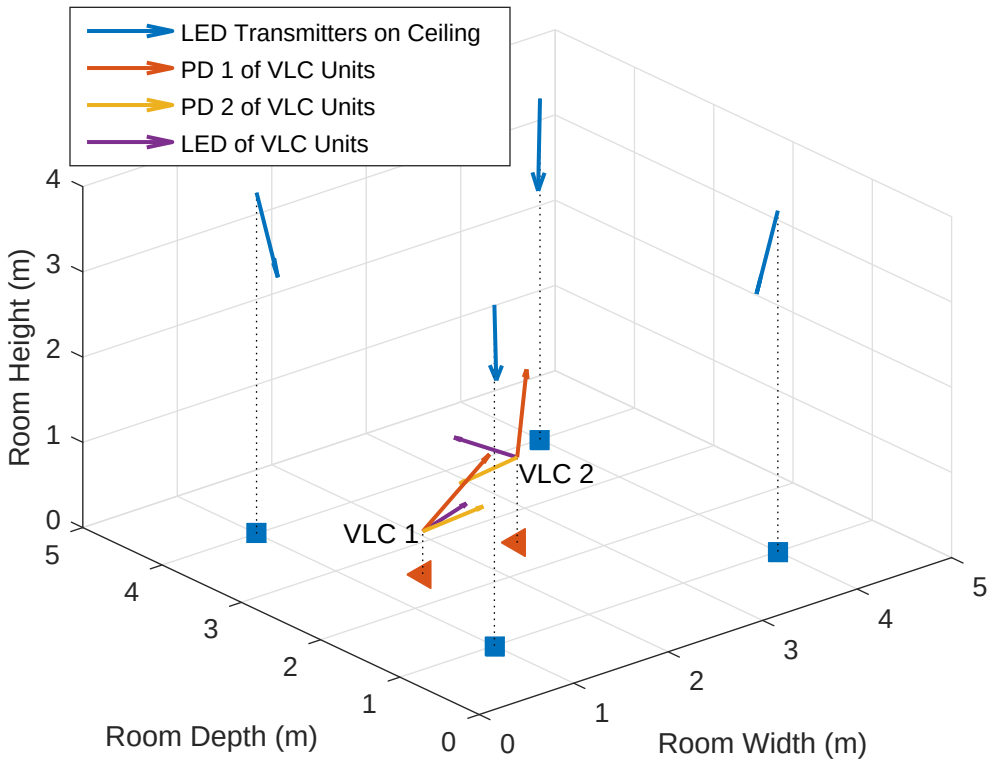

Figure 4.2: VLP network configuration in the simulations. Each VLC unit contains two PDs and one LED. PD 1 of the VLC units is used to obtain measurements from the LEDs on the ceiling while PD 2 of the VLC units communicates with the LED of the other VLC unit for cooperative localization. The squares and the triangles show the projections of the LEDs and the VLC units on the floor, respectively.

In order to analyze the localization performance of the VLC units with respect to the transmit powers of the LEDs on the ceiling (equivalently, anchors), individual CRLBs for localization of the VLC units in noncooperative and cooperative scenarios are plotted against the transmit powers of LEDs on the ceiling

in Fig. 4.3, where the transmit power of the VLC units is fixed to 1 W. As observed from Fig. 4.3, the CRLBs in the cooperative scenario converge to those in the noncooperative scenario as the transmit powers of the LEDs increase. Since the first (second) summand in the FIM expression in (2.19) corresponds to the noncooperative (cooperative) localization, higher transmit powers of the LEDs on the ceiling cause the first summand to be much greater than the second summand, which makes the contribution of cooperation to the FIM negligible. Hence, the effect of cooperation on localization performance becomes less significant as the transmit power increases, which is in compliance with the results obtained for RF based cooperative localization networks [9]. In addition, it is observed from Fig. 4.3 that the improvement in localization accuracy gained by employing cooperation among the VLC units is higher for VLC 2 as compared to that for VLC 1. This is an intuitive result since the localization of VLC 2 depends mostly on LED 2 (the other LEDs are not sufficiently close to facilitate the localization process), and incorporating cooperative measurements for VLC 2 provides an improvement in localization performance that is much greater than that for VLC 1, which can obtain informative measurements from the LEDs on the ceiling even in the absence of cooperation.

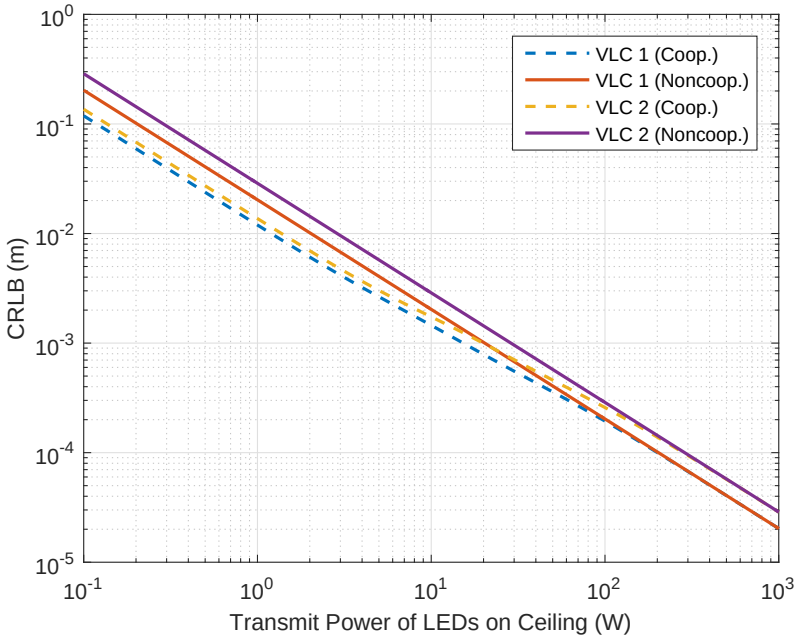

Figure 4.3: Individual CRLBs for localization of VLC units in both noncooperative and cooperative cases with respect to the transmit power of LEDs on ceiling, where the transmit power of VLC units is taken as 1W.

Finally, the localization performance of the VLC units is investigated with respect to the transmit powers of the VLC units when the transmit powers of the LEDs on the ceiling are fixed. Fig. 4.4 illustrates the CRLBs for localization of the VLC units versus the transmit powers of the VLC units in the noncooperative and cooperative cases. As observed from Fig. 4.4, cooperation leads to a higher improvement in the performance of VLC 2, similar to Fig. 4.3. In addition, via the FIM expression in (2.19), it can be noted that the contribution of cooperation to localization performance gets higher as the transmit powers of the VLC units increase, which is also observed from Fig. 4.4. However, the CRLB reaches a saturation level above a certain power threshold, as opposed to Fig. 4.3, where the CRLB continues to decrease as the power increases. The main reason for this distinction between the effects of the transmit powers of the LEDs on the ceiling and those of the VLC units can be explained as follows: For a fixed transmit power of the VLC units, the localization error in a three-dimensional scenario by using

four anchors (i.e., four LEDs on the ceiling) converges to zero as the transmit powers of the anchors increase regardless of the existence of cooperation. On the other hand, for a fixed transmit power of the LEDs on the ceiling, increasing the transmit power of the VLC unit (i.e., one of the anchors) cannot reduce the localization error below a certain level. Therefore, the saturation level represents the localization accuracy that can be attained by five anchors with four anchors leading to noisy RSS measurements and one anchor generating noise-free RSS measurements.

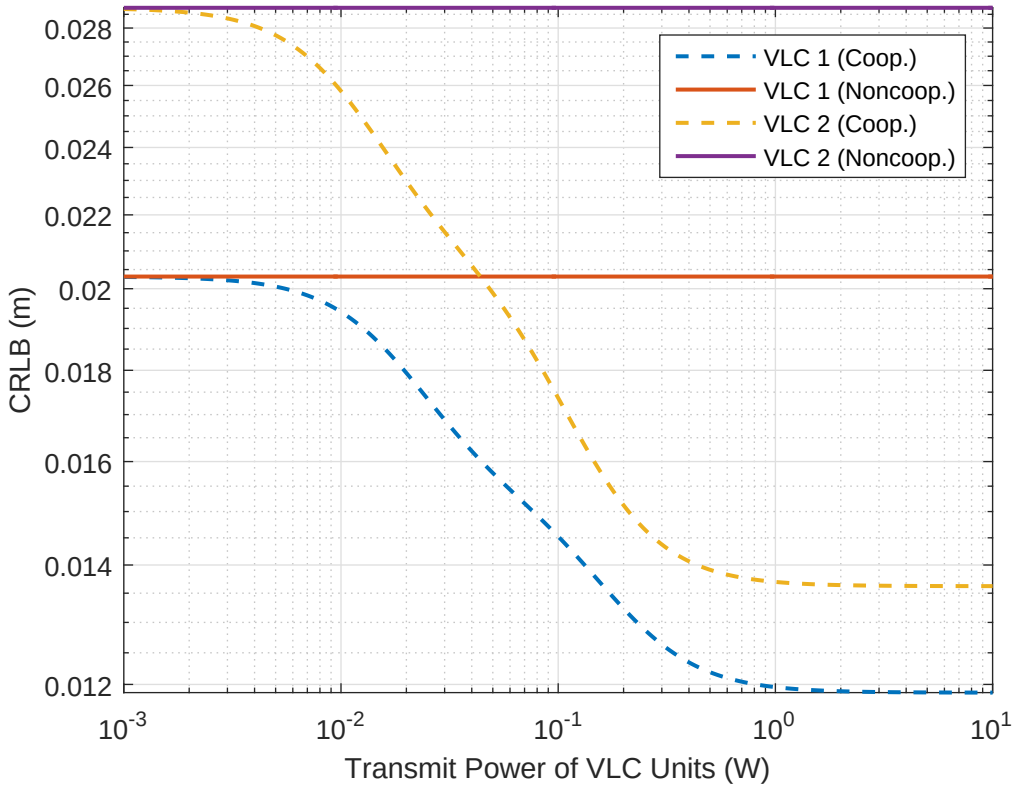

Figure 4.4: Individual CRLBs for localization of VLC units in both noncooperative and cooperative cases with respect to the transmit power of VLC units, where the transmit power of LEDs on ceiling is taken as 1W.

4.2 Scenario 2: 4 VLC Unit, 1 Cooperating Element

In this scenario, 4 VLC units are located at $\mathbf{x}_1 = [1.5\ 1.5\ 0.5]^T$m, $\mathbf{x}_2 = [3.5\ 1.5\ 0.5]^T$m, $\mathbf{x}_3 = [3.5\ 3.5\ 0.5]^T$m and $\mathbf{x}_4 = [1.5\ 3.5\ 0.5]^T$m as in Fig. 4.5. Since the VLC units are at the same horizontal and vertical distance to the closest LED, noncooperative CRLB values are expected to be equal. In this scenario, there exist 1 PD and 1 LED for cooperation. In this specific case, the connectivity sets are defined so that the cooperating PD of VLC unit 1 (VLC-U-1) is connected to the cooperating LEDs of VLC-U-2 and VLC-U-3. There exist no more connections in the cooperative case.

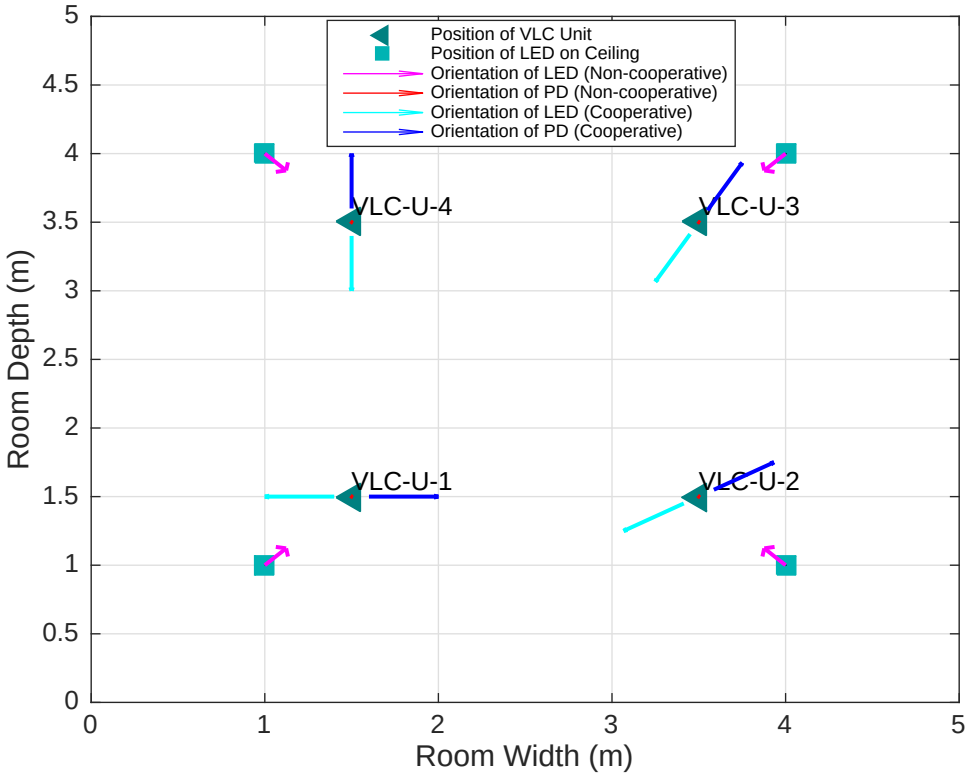

Figure 4.5: 4 VLC units each with 1 cooperating LED and PD (top view).

In Fig. 4.6, it can be seen that noncooperative CRLB values are the same for

each VLC unit. In the cooperative case, VLC-U-1 has the best performance since it is connected to two other VLC units. VLC-U-2's performance is slightly better than VLC-U-3's since it can provide higher power to VLC-U-1 than VLC-U-3.

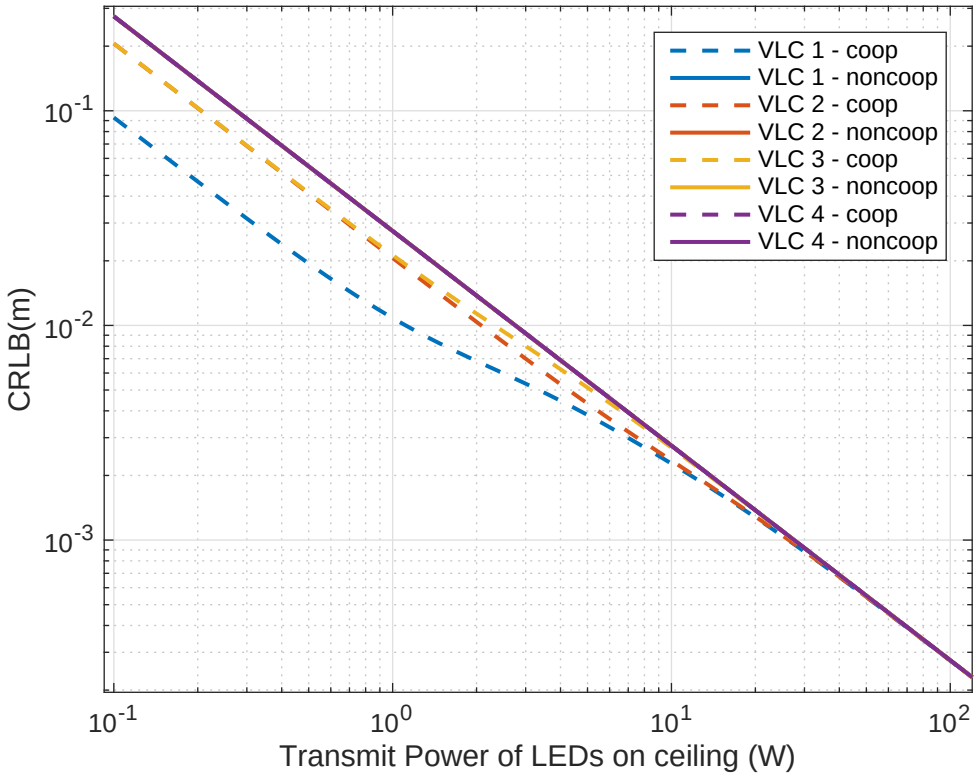

Figure 4.6: 4 VLC units each with 1 cooperating LED and PD. Transmit powers of LEDs on VLC units are 1 W.

In Fig. 4.7, after some transmit power value of VLC units, VLC-U-2 and VLC-U-3 provide the same CRLB values since both are connected to one VLC unit. VLC-U-1 again provides the best performance due to its connection to two other units.

It is noted that VLC-U-2 and VLC-U-3 do not get any power from their cooperating PDs; they can just provide power to the cooperating PDs of VLC-U-1. This case does not prevent improvements in localization performance since the relative distance is used for both connected units.

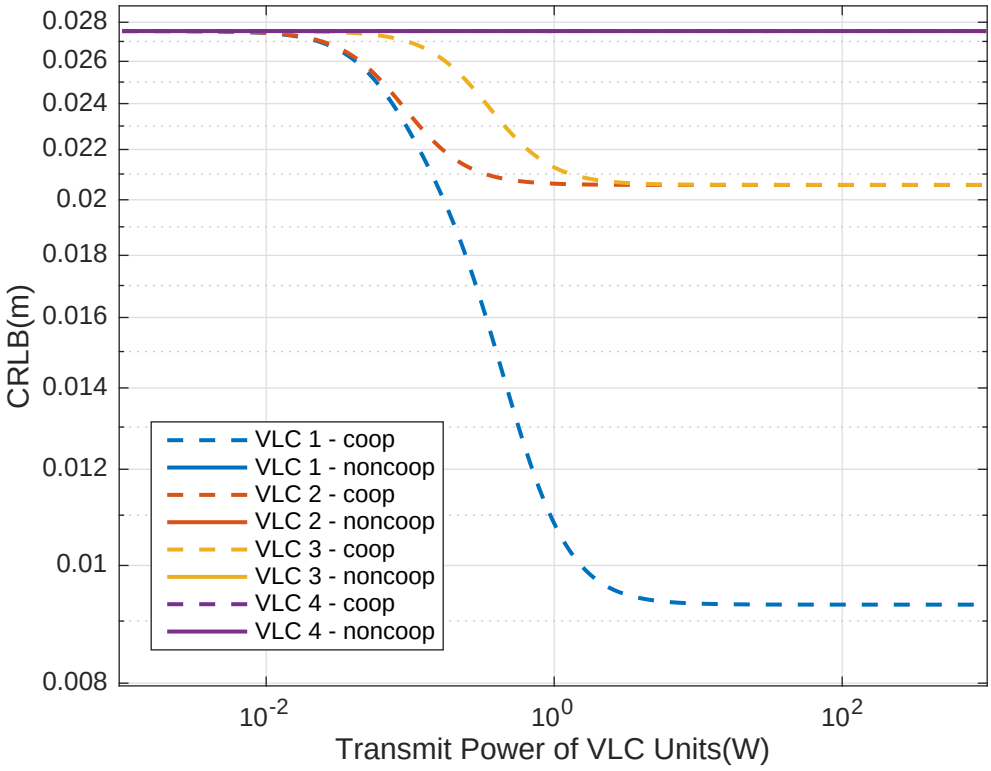

Figure 4.7: 4 VLC units each with 1 cooperating LED and PD. Transmit powers of LEDs on the ceiling are 1 W.

4.3 Scenario 3: 3 VLC Unit, 1 Cooperating Element

In this scenario, 4 VLC units are located at $\mathbf{x}_1 = [3\ 2\ 0.5]^T$m, $\mathbf{x}_2 = [2\ 1\ 0.5]^T$m and $\mathbf{x}_3 = [1\ 4\ 0.5]^T$m as in Fig. 4.8. In this scenario, the connectivity sets are defined so that the connecting PD of VLC-U-2 is connected to the cooperating LEDs of VLC-U-1 and VLC-U-3. There are no more connections in the cooperative case.

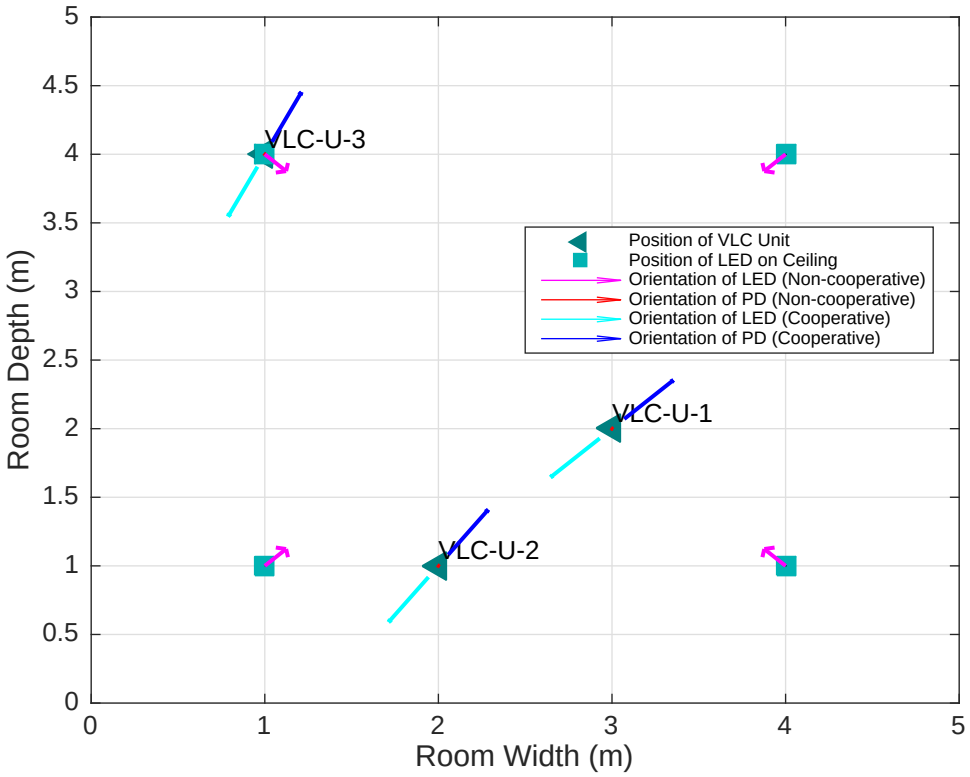

Figure 4.8: 3 VLC units each with 1 cooperating LED and PD (top view).

In Fig. 4.9, it can be seen that VLC-U-2 provides the best cooperative localization performance since it is connected to two other VLC units. Its performance becomes even better than VLC-U-1, which has higher noncooperative positioning performance. In this plot, it can be observed that, for all VLC units, cooperative

CRLB values are stable after some point. After that point, increasing the powers of LEDs on VLC units does not provide any performance improvement.

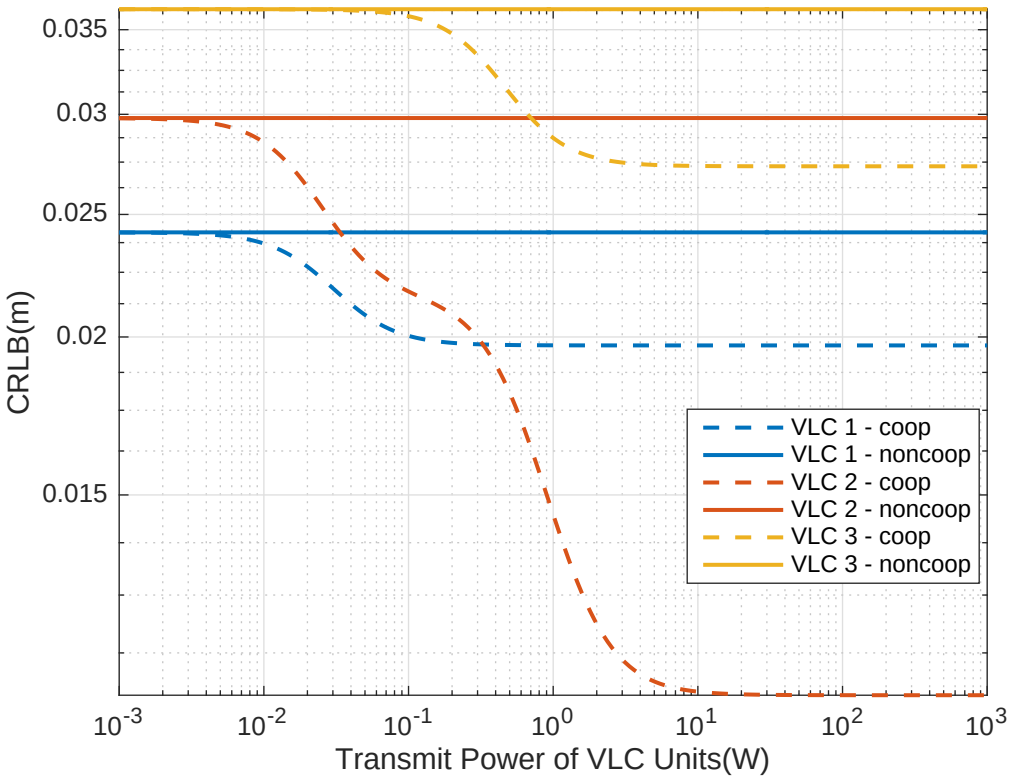

Figure 4.9: 3 VLC units each with 1 cooperating LED and PD. Transmit power of LEDs on the ceiling are 1 W.

4.4 Scenario 4: 3 VLC Unit, 6 Cooperating Element

In this scenario, 4 VLC units are located in $\mathbf{x}_1 = [3\ 2\ 0.5]^T$m, $\mathbf{x}_2 = [2\ 1\ 0.5]^T$m and $\mathbf{x}_3 = [1\ 4\ 0.5]^T$m as in Fig. 4.10. There are 6 cooperating elements in this scenario. After obtaining the connectivity sets, it is noted that there are 12 connections in total and each VLC unit is a part of 8 connections.

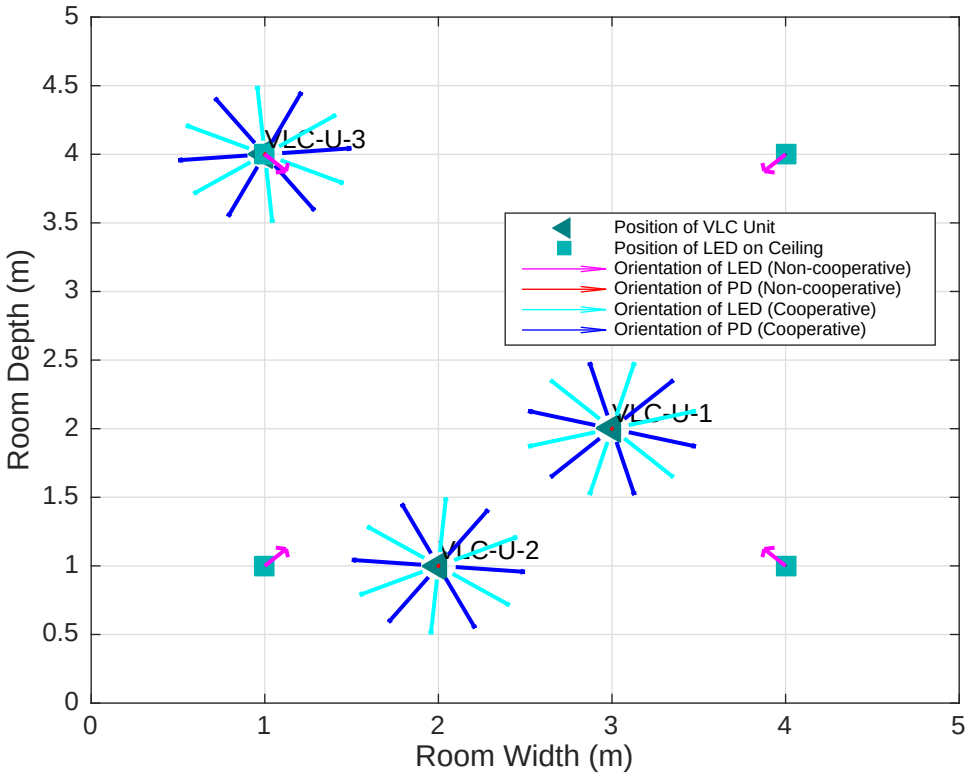

Figure 4.10: 3 VLC units each with 1 cooperating LED and PD (top view).

In Fig. 4.11, it is observed that VLC-U-3 provides the best cooperative localization performance even though its noncooperative positioning performance is the worst among the others. An intiutive explanation of this case can be provided as follows: VLC-U-1 is the closest one to the center but the furthest one to the LEDs on average. When the transmit power of the LEDs at the VLC units is

increased, after some level, power coming from the LEDs on the ceiling generates the performance differences. VLC-U-3 is very close to one of those LEDs; therefore, it has the minimum CRLB in the cooperative case.

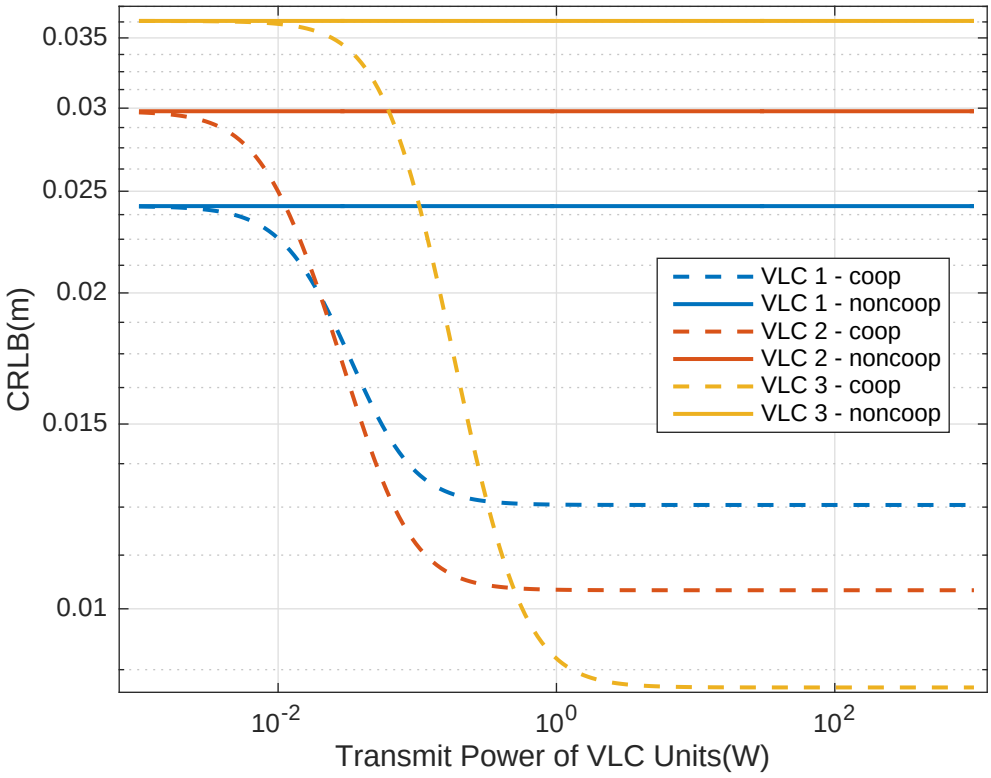

Figure 4.11: 3 VLC units each with 1 cooperating LED and PD. Transmit powers of LEDs on the ceiling are 1 W.

Chapter 5

Simulation Results for Performance Evaluation of Sequential Estimator

In this chapter, the performance of the sequential algorithm, which is proposed in Chapter 3, is investigated.

5.1 Scenario 1: 3 VLC-Units

To evaluate the performance of the sequential estimation algorithm, the system shown in Fig. 5.1 is used. A room of size 10m×10m×5m is considered, where there exist $N_L = 4$ LED transmitters on the ceiling which are located at $\mathbf{y}_1 = [1\ 1\ 5]^T$m, $\mathbf{y}_2 = [1\ 9\ 5]^T$m, $\mathbf{y}_3 = [9\ 1\ 5]^T$m, and $\mathbf{y}_4 = [9\ 9\ 5]^T$m. The orientations of the LEDs on the ceiling are adjusted so that each LED is directed towards the center of the room with an offset angle of 5° with respect to the normal vector of the ceiling. There are $N_V = 3$ VLC units in the system, located at $\mathbf{x}_1 = [7\ 8\ 0]^T$m, $\mathbf{x}_2 = [3\ 3\ 0]^T$m and $\mathbf{x}_3 = [7.2\ 0.8\ 0]^T$m.

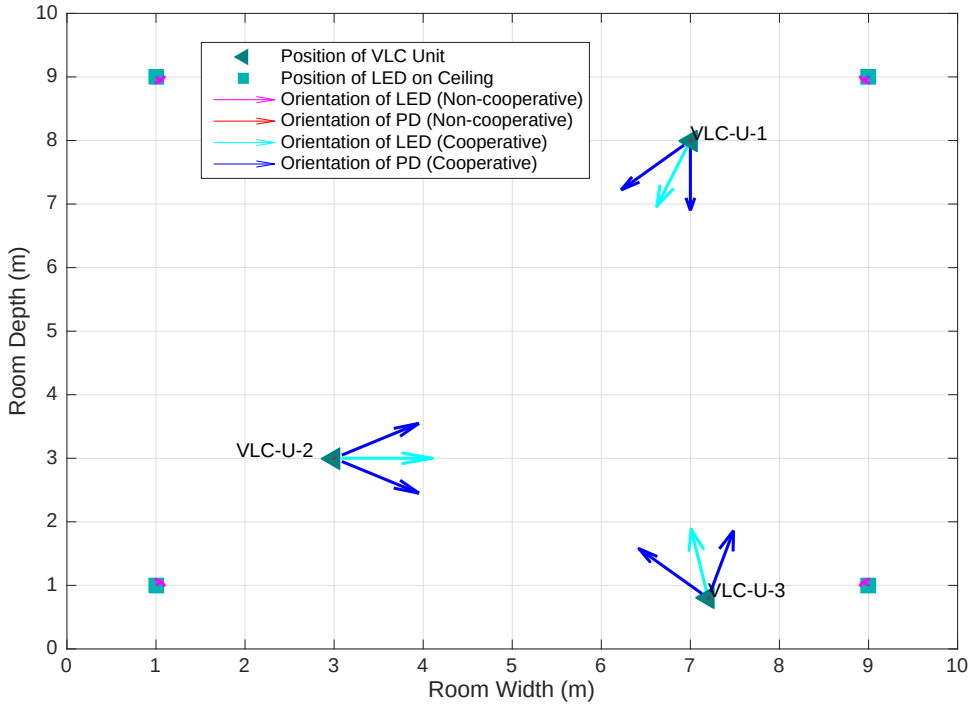

Figure 5.1: Top view of VLP network configuration for performance evaluation of sequential estimator. The squares and the triangles show the projections of the LEDs on the ceiling and the VLC units on the floor, respectively.

Each VLC unit contains three PDs and one LED. PD 1 of each VLC unit is used to obtain measurements from the LEDs on the ceiling and it points upwards. The location of this PD for each VLC unit is 10 cm higher than the center point of the VLC unit. PD 2 and PD 3 of the VLC units communicate with the LEDs of the other VLC units for cooperative positioning. The PDs and LEDs that are used for cooperation are located on a circle, having the VLC unit position as the center point with a radius of 10 cm. The normal vectors of cooperating PDs and LEDs are chosen according to their positions so that they point outwards. The FOVs of the PDs are taken as 75° and the area of each PD is 1 cm^2. Furthermore, $S_k^{(i,j)}$ values in (2.2) are shown in Table 5.1. For i, j, k values that do not appear in the table, the connectivity sets are empty. Also, $\widetilde{S}_1^{(j)} = \{1, 2, 3, 4\}$, and $\widetilde{S}_k^{(j)} = \emptyset$ for $k \in \{2, 3\}$ and all $j \in \{1, 2, 3\}$ in the noncooperative case.

Table 5.1: $S_k^{(i,j)}$ values for the scenario shown in Fig. 5.1

$S_k^{(i,j)}$	$(i,\ j)$						
		1,2	**1,3**	**2,1**	**2,3**	**3,1**	**3,2**
k	**2**	1	1	1	Ø	1	Ø
	3	Ø	1	Ø	1	1	1

The *globalsearch* function of MATLAB is used for solving the optimization problem in (3.1). The RMSE of the sequential estimator is computed considering 500 Monte-Carlo trials. In Fig. 5.2, the RMSEs of the sequential estimator are plotted together with the CRLBs in the presence and absence of cooperation.

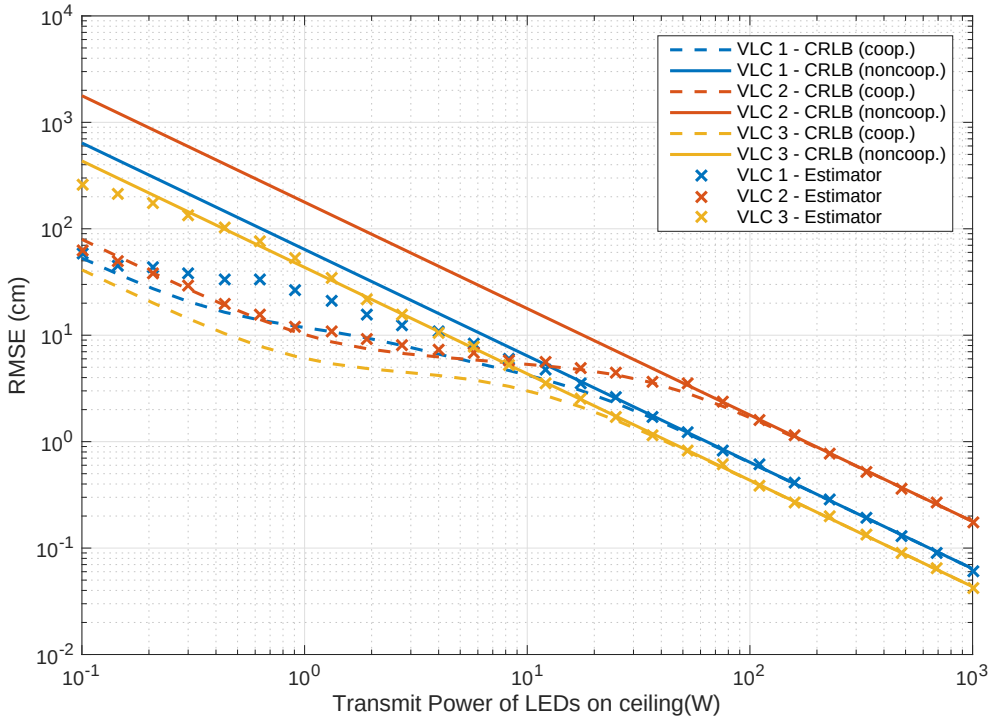

Figure 5.2: RMSE of the sequential estimator and CRLBs versus transmit power of LEDs on ceiling. In the sequential positioning algorithm, localization order is VLC-U-3, VLC-U-1 and VLC-U-2. Transmit powers of LEDs on VLC units are 1 W.

In this scenario, the sequential positioning algorithm estimates the position of VLC-U-3 first since the noncooperating PD of it measures the highest total power among all VLC units. As a result, the RMSE of the sequential estimator for VLC-U-3 achieves the noncooperative CRLB. Then, the sequential algorithm estimates the location of VLC-U-1 based on the signals from the LEDs on the ceiling and from VLC-U-3. Finally, the location of VLC-U-2 is estimated based on the signals from the other VLC units and the LEDs on the ceiling. It is noted that the RMSEs for VLC-U-2 are very close to the cooperative CRLB since cooperation is utilized effectively in that case.

For high SNR values, effects of the cooperation are not observed and the cooperative CRLB converges to the noncooperative CRLB. It is observed that the sequential estimator achieves cooperative / noncooperative CRLB at high SNRs. In particuar, the RMSEs of the sequential estimator for VLC-U-1 and VLC-U-2 follow cooperative CRLB values as the transmit power of the LEDs in the ceiling increases. However, there is a region around 1 Watt of transmit power where the sequential estimator does not achieve the CRLB for VLC-U-1, as it does for VLC-U-2. The reason is that the sequential positioning algorithm estimates the position of VLC-U-1 without any cooperation from VLC-U-2. However, VLC-U-2 utilizes the cooperation of both VLC units during position estimation.

5.2 Scenario 2: 3 VLC-Units

In this example, the scenario in Fig. 5.3 is used. A room of size 8m×8m×5m is considered, where there exist $N_L = 4$ LED transmitters on the ceiling that are located at $\mathbf{y}_1 = [1\ 1\ 5]^T$m, $\mathbf{y}_2 = [1\ 7\ 5]^T$m, $\mathbf{y}_3 = [7\ 1\ 5]^T$m, and $\mathbf{y}_4 = [7\ 7\ 5]^T$m. The LEDs on the ceiling point downwards, without any tilt angle, i.e., with normal vectors $[0\ 0\ -1]^T$. There are $N_V = 3$ VLC units in the system, located at $\mathbf{x}_1 = [1\ 2\ 0]^T$m, $\mathbf{x}_2 = [3\ 4\ 0]^T$m and $\mathbf{x}_3 = [5\ 3\ 0]^T$m.

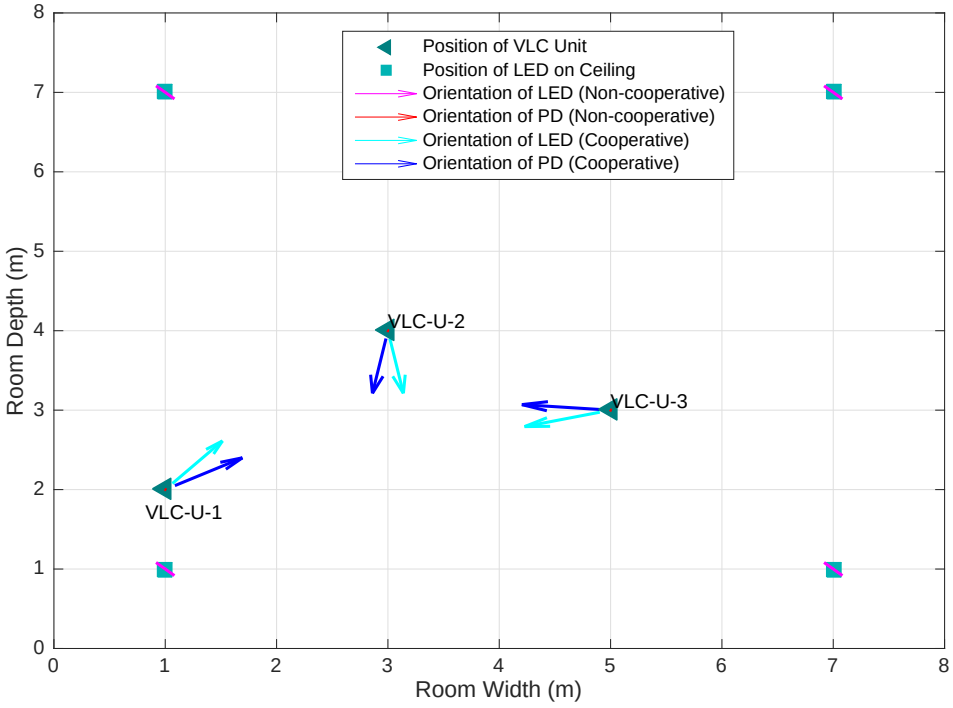

Figure 5.3: Top view of the VLP network configuration for performance evaluation of the sequential estimator. The squares and the triangles show the projections of the LEDs on the ceiling and the VLC units on the floor, respectively.

Each VLC unit contains two PDs and one LED. The PDs with index 1 of the VLC units are used to obtain measurements from the LEDs on the ceiling. These PDs point upwards and are located 10 cm higher than the center point of the VLC units. The PDs with index 2 of the VLC units communicate with the LEDs

of the other VLC units for cooperative positioning. The PDs and LEDs that are used for cooperation are located on a circle. The center of the circle is the position of the VLC unit and the radius of the circle is 10 cm for both VLC units. The normal vectors of the cooperating PDs and LEDs are chosen according to their positions in such a way that they point outwards with respect to the center. The FOV of each PD is 60° and the area of each PD is 1 cm^2. Furthermore, $S_k^{(i,j)}$ values are shown in Table 5.2. For i, j, k values that do not appear in the table, the connectivity sets are empty. Also, $\widetilde{S}_1^{(j)} = \{1, 2, 3, 4\}$, and $\widetilde{S}_2^{(j)} = \emptyset$ for all $j \in \{1, 2, 3\}$.

Table 5.2: $S_k^{(i,j)}$ values for the scenario shown in Fig. 5.3

$S_k^{(i,j)}$	*(i, j)*						
k		**1,2**	**1,3**	**2,1**	**2,3**	**3,1**	**3,2**
	2	1	1	1	1	1	Ø

The RMSE of the sequential estimator is computed with 300 Monte-Carlo trials. In Fig. 5.4, the RMSEs of the sequential estimator are illustrated together with the CRLBs in the presence and absence of cooperation.

In this scenario, VLC-U-3 is chosen to be first location estimation unit, that is, the sequential positioning algorithm estimates the position of VLC-U-3 first. As a result, the RMSE of the sequential estimator for VLC-U-3 achieves the noncooperative CRLB.

Cooperation is utilized for VLC-U-1 and VLC-U-2. The RMSE values for those VLC units follow noncooperative CRLB values for different transmit power of LEDs on the VLC units.

Then, the sequential algorithm estimates the location of VLC-U-1, based on the signals from the LEDs on the ceiling and from VLC-U-3. After that, the location of VLC-U-2 is estimated based on the signals from other both VLC units and the LEDs on the ceiling. It is noted that the RMSEs for VLC-U-2 are close to the cooperative CRLB since cooperation is utilized effectively in that

case. The RMSEs for VLC-U-1 are close to the cooperating CRLB until 100 mW power. For higher LED power values, the cooperative CRLB values decrease but the RMSEs keep a certain level.

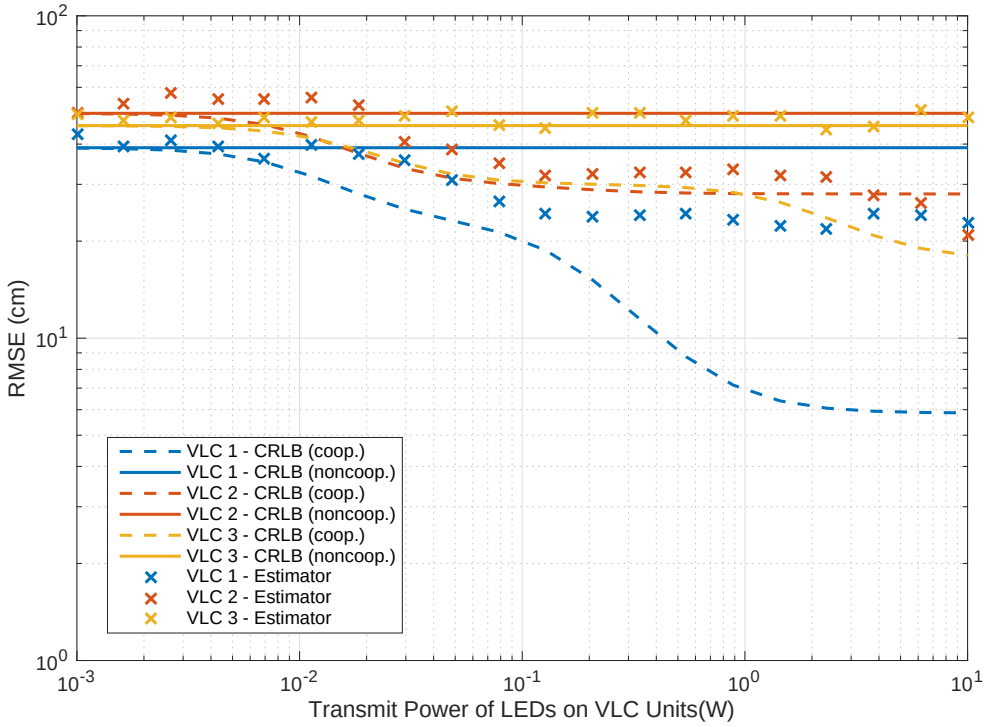

Figure 5.4: RMSE of the sequential estimator and CRLBs versus transmit power of LEDs on ceiling. In sequential positioning algorithm, localization order is VLC-U-3, VLC-U-1 and VLC-U-2. Transmit powers of LEDs on the ceiling are 500 mW.

Changing the transmit power of the LEDs on the VLC units has no effect in the noncooperative case; therefore the noncooperative CRLB values are constant for each VLC unit as in Fig. 5.4. When the transmit power of the LEDs on VLC the units are very low, cooperation does not improve the localization accuracy. As can be noted from Fig. 5.4, if the transmit power of the LEDs on the VLC units are around 1 mW or less, cooperative and noncooperative CRLB values are very close to each other. The RMSE values of the sequential estimator also show

the same behavior.

The effects of cooperation on the localization performance are more significant when the transmit power of cooperating LEDs is above 100 mW. In the non-cooperative case, the CRLB values are around 40 cm. In the cooperative case, with 1 W LEDs on the VLC units, around 20 cm improvement is achieved for VLC-U-2 and VLC-U-3. For VLC-U-1, the improvement is even more, but the theoretical bound is not achieved since the only cooperation is with VLC-U-3 while estimating the position of VLC-U-1. (The location of VLC-U-2 is unknown at that instant.) However, while calculating the CRLB values for the cooperative case, full utilization of cooperation is considered.

5.3 Scenario 3: 3 VLC-Units

To evaluate the performance of the sequential estimation algorithm, the system shown in Fig. 5.5 is used. A room of size 8m×8m×5m is considered, where there exist $N_L = 4$ LED transmitters on the ceiling which are located at $\mathbf{y}_1 = [1\ 1\ 5]^T$m, $\mathbf{y}_2 = [1\ 7\ 5]^T$m, $\mathbf{y}_3 = [7\ 1\ 5]^T$m, and $\mathbf{y}_4 = [7\ 7\ 5]^T$m. The orientations of the LEDs on the ceiling are adjusted so that each LED is directed towards the center of the room with an offset angle of 5° with respect to the normal vector of the ceiling. There are $N_V = 3$ VLC units in the system, located at $\mathbf{x}_1 = [6\ 5.5\ 1.5]^T$m, $\mathbf{x}_2 = [4\ 2.5\ 1.5]^T$m and $\mathbf{x}_3 = [6.1\ 0.8\ 1.5]^T$m.

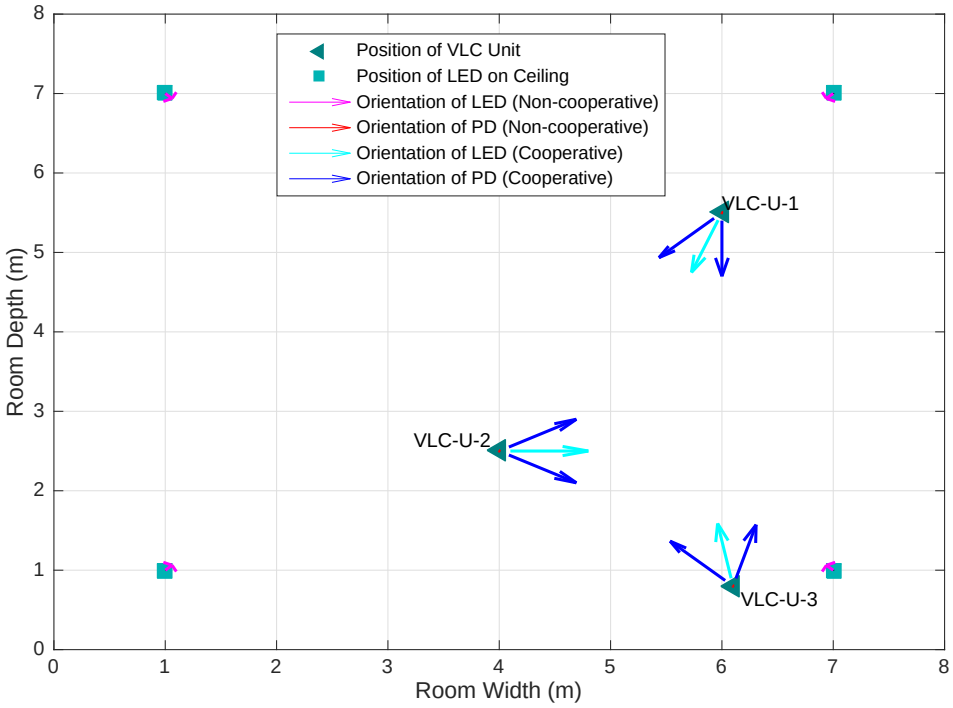

Figure 5.5: Top view of VLP network configuration for performance evaluation of the sequential estimator. The squares and the triangles show the projections of the LEDs on the ceiling and the VLC units on the floor, respectively.

Each VLC unit contains three PDs and one LED. PD 1 of each VLC unit is used to obtain measurements from the LEDs on the ceiling. These PDs point

upwards and are located 10 cm higher than the center point of the VLC units. PD 2 and PD 3 of the VLC units communicate with the LEDs of the other VLC units for cooperative positioning. The PDs and LEDs which are used for cooperation are located on a circle, having VLC unit position as the center point with a radius of 10 cm. The normal vectors of the cooperating PDs and LEDs are chosen according to their positions so that they point outwards. The FOV of each PD is 75° and the area of each PD is 1 cm^2. Furthermore, $S_k^{(i,j)}$ values are shown in Table 5.1. For i, j, k values that do not appear in the table, the connectivity sets are empty. In addition, $\widetilde{S}_1^{(j)} = \{1, 2, 3, 4\}$, and $\widetilde{S}_k^{(j)} = \emptyset$ for $k \in \{2, 3\}$ and all $j \in \{1, 2, 3\}$ in the noncooperative case.

Table 5.3: $S_k^{(i,j)}$ values for the scenario shown in Fig. 5.5

$S_k^{(i,j)}$	*(i, j)*						
		1,2	**1,3**	**2,1**	**2,3**	**3,1**	**3,2**
k	**2**	1	1	1	Ø	1	Ø
	3	Ø	1	1	1	1	1

The RMSE of the sequential estimator is computed with 300 Monte-Carlo trials. In Fig. 5.6, the RMSEs of the sequential estimator are illustrated together with the CRLBs in the presence and absence of cooperation.

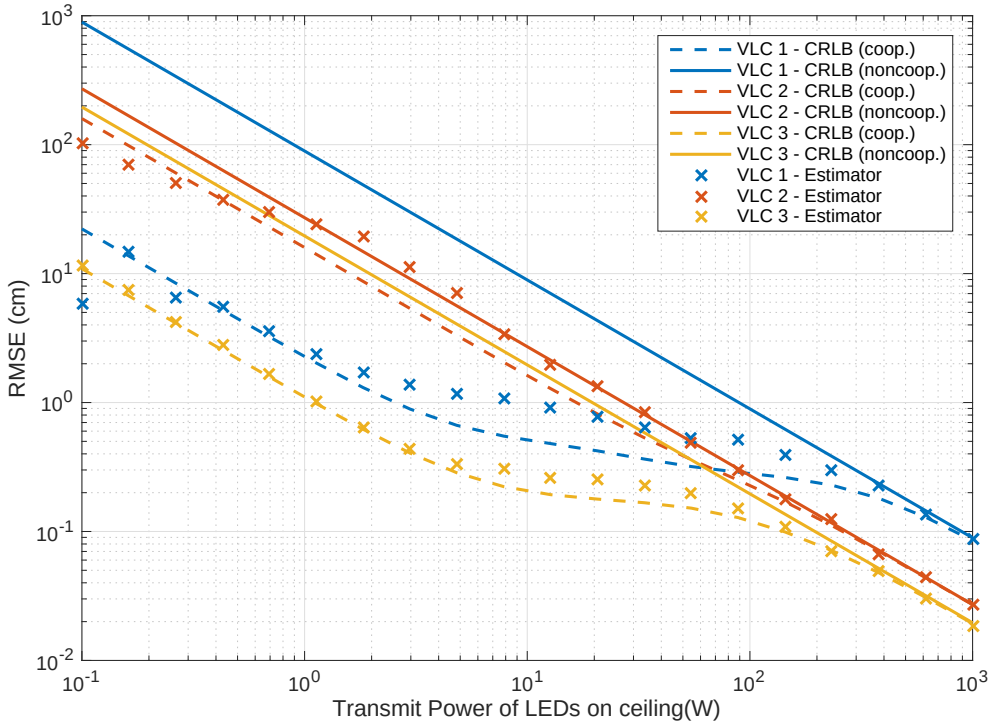

Figure 5.6: RMSE of the sequential estimator and CRLBs versus transmit power of LEDs on ceiling. In the sequential positioning algorithm, localization order is VLC-U-2, VLC-U-3 and VLC-U-1. Transmit powers of LEDs on the VLC units are 5 W.

In this scenario, VLC-U-2 is chosen to be first location estimation unit; that is, the sequential positioning algorithm estimates the position of VLC-U-2 first. As a result, the RMSE of the sequential estimator for VLC-U-2 achieves the noncooperative CRLB. Cooperation is utilized for VLC-U-1 and VLC-U-3.

At high SNRs, the effects of cooperation are not observed and the cooperative CRLB converges to the noncooperative one. With 500 mW transmit power of LEDs on the ceiling, having a 5 W LED for cooperation improves the performance of the system significantly. The sequential estimator achieves the CRLBs for all VLC units.

Chapter 6

Concluding Remarks and Future Work

In this thesis, a cooperative VLP system has been proposed. In the proposed system, there are N_L LEDs on the ceiling, with known locations and orientation vectors, and N_V VLC units at unknown locations. Each VLC unit contains multiple LEDs and multiple PDs, whose relative positions on the VLC units and orientation vectors are also known. Connectivity sets have been defined to specify cooperations among VLC units by determining the presence/absence of a connection between any LED and PD in the system. An RSS based, generic CRLB expression is derived for cooperative location estimation of VLC units, covering noncooperative scenario as a special case. A low complexity sequential positioning algorithm is proposed and its performance is evaluated in various scenarios. It has been observed that the RMSE values achieved by the sequential positioning algorithm are close to the CRLB under certain conditions.

As future work, an experimental study will be conducted for performance evaluation of the algorithm in various practical scenarios, varying the number of LEDs and the positions and orientations of LEDs and PDs at VLC units. The sequential positioning algorithm will be improved by investigating the optimal way of setting the estimation order. A dynamic estimation order selection approach will

be studied by running the sequential positioning algorithm multiple times and adapting the estimation order each time.

Bibliography

[1] G. Mao and B. Fidan, *Localization Algorithms and Strategies for Wireless Sensor Networks*. Information Science Reference, 2009.

[2] K. Pahlavan and P. Krishnamurthy, *Principles of Wireless Access and Localization*. Wiley Desktop Editions, Wiley, 2013.

[3] H. Liu, H. Darabi, P. Banerjee, and J. Liu, "Survey of wireless indoor positioning techniques and systems," *IEEE Transactions on Systems, Man, and Cybernetics, Part C (Applications and Reviews)*, vol. 37, pp. 1067–1080, Nov. 2007.

[4] M. Cypriani, F. Lassabe, P. Canalda, and F. Spies, "Wi-Fi-based indoor positioning: Basic techniques, hybrid algorithms and open software platform," in *International Conference on Indoor Positioning and Indoor Navigation (IPIN)*, Sep. 2010.

[5] Z. Sahinoglu, S. Gezici, and I. Guvenc, *Ultra-wideband Positioning Systems: Theoretical Limits, Ranging Algorithms, and Protocols*. New York: Cambridge University Press, 2008.

[6] J. Armstrong, Y. Sekercioglu, and A. Neild, "Visible light positioning: A roadmap for international standardization," *IEEE Communications Magazine*, vol. 51, pp. 68–73, Dec. 2013.

[7] J. Grubor, S. Randel, K. D. Langer, and J. W. Walewski, "Broadband information broadcasting using led-based interior lighting," *Journal of Lightwave Technology*, vol. 26, pp. 3883–3892, Dec. 2008.

[8] D. Karunatilaka, F. Zafar, V. Kalavally, and R. Parthiban, "Led based indoor visible light communications: State of the art," *IEEE Communications Surveys Tutorials*, vol. 17, pp. 1649–1678, thirdquarter 2015.

[9] M. R. Gholami, M. F. Keskin, S. Gezici, and M. Jansson, *Cooperative Positioning in Wireless Networks*, pp. 1–19. Wiley Encyclopedia of Electrical and Electronics Engineering, 2016.

[10] R. M. Vaghefi, M. R. Gholami, R. M. Buehrer, and E. G. Strom, "Cooperative received signal strength-based sensor localization with unknown transmit powers," *IEEE Transactions on Signal Processing*, vol. 61, pp. 1389–1403, Mar. 2013.

[11] A. Conti, M. Guerra, D. Dardari, N. Decarli, and M. Z. Win, "Network experimentation for cooperative localization," *IEEE Journal on Selected Areas in Communications*, vol. 30, pp. 467–475, Feb. 2012.

[12] Y. Shen, H. Wymeersch, and M. Z. Win, "Fundamental limits of wideband cooperative localization via Fisher information," in *IEEE Wireless Commun. and Networking Conf.*, pp. 3951–3955, Mar. 2007.

[13] C. L. F. Mayorga, F. della Rosa, S. A. Wardana, G. Simone, M. C. N. Raynal, J. Figueiras, and S. Frattasi, "Cooperative positioning techniques for mobile localization in 4G cellular networks," in *IEEE International Conference on Pervasive Services*, pp. 39–44, July 2007.

[14] E. D. Nerurkar, S. I. Roumeliotis, and A. Martinelli, "Distributed maximum a posteriori estimation for multi-robot cooperative localization," in *IEEE International Conference on Robotics and Automation*, pp. 1402–1409, May 2009.

[15] R. M. Vaghefi and R. M. Buehrer, "Joint TOA-based sensor synchronization and localization using semidefinite programming," in *IEEE Int. Conference on Commun. (ICC)*, pp. 520–525, June 2014.

[16] M. R. Gholami, S. Gezici, and E. G. Strom, "Improved position estimation using hybrid TW-TOA and TDOA in cooperative networks," *IEEE Transactions on Signal Processing*, vol. 60, pp. 3770–3785, July 2012.

[17] H. Wymeersch, J. Lien, and M. Z. Win, "Cooperative localization in wireless networks," *Proceedings of the IEEE*, vol. 97, pp. 427–450, Feb. 2009.

[18] M. R. Gholami, L. Tetruashvili, E. G. Strom, and Y. Censor, "Cooperative wireless sensor network positioning via implicit convex feasibility," *IEEE Transactions on Signal Processing*, vol. 61, pp. 5830–5840, Dec. 2013.

[19] T. Wang, Y. Sekercioglu, A. Neild, and J. Armstrong, "Position accuracy of time-of-arrival based ranging using visible light with application in indoor localization systems," *Journal of Lightwave Technology*, vol. 31, pp. 3302–3308, Oct. 2013.

[20] X. Zhang, J. Duan, Y. Fu, and A. Shi, "Theoretical accuracy analysis of indoor visible light communication positioning system based on received signal strength indicator," *Journal of Lightwave Technology*, vol. 32, pp. 4180–4186, Nov. 2014.

[21] M. F. Keskin and S. Gezici, "Comparative theoretical analysis of distance estimation in visible light positioning systems," *Journal of Lightwave Technology*, vol. 34, pp. 854–865, Feb. 2016.

[22] M. F. Keskin, E. Gonendik, and S. Gezici, "Improved lower bounds for ranging in synchronous visible light positioning systems," *Journal of Lightwave Technology*, vol. 34, pp. 5496–5504, Dec. 2016.

[23] E. Gonendik and S. Gezici, "Fundamental limits on RSS based range estimation in visible light positioning systems," *IEEE Communications Letters*, vol. 19, pp. 2138–2141, Dec. 2015.

[24] A. Sahin, Y. S. Eroglu, I. Guvenc, N. Pala, and M. Yuksel, "Hybrid 3-D localization for visible light communication systems," *Journal of Lightwave Technology*, vol. 33, pp. 4589–4599, Nov. 2015.

[25] H. Steendam, T. Q. Wang, and J. Armstrong, "Theoretical lower bound for indoor visible light positioning using received signal strength measurements and an aperture-based receiver," *Journal of Lightwave Technology*, vol. 35, pp. 309–319, Jan. 2017.

[26] O. Erdem, M. F. Keskin, and S. Gezici, "Effects of cooperation on visible light positioning," in *2017 IEEE International Black Sea Conference on Communications and Networking (BlackSeaCom)*, June 2017.

[27] M. Yasir, S. W. Ho, and B. N. Vellambi, "Indoor positioning system using visible light and accelerometer," *Journal of Lightwave Technology*, vol. 32, pp. 3306–3316, Oct. 2014.

[28] L. Li, P. Hu, C. Peng, G. Shen, and F. Zhao, "Epsilon: A visible light based positioning system," in *11th USENIX Symposium on Networked Systems Design and Implementation*, (Seattle, WA), pp. 331–343, 2014.

[29] H. V. Poor, *An Introduction to Signal Detection and Estimation*. New York: Springer-Verlag, 1994.

[30] H. Ma, L. Lampe, and S. Hranilovic, "Coordinated broadcasting for multiuser indoor visible light communication systems," *IEEE Transactions on Communications*, vol. 63, pp. 3313–3324, Sep. 2015.

[31] T. Komine and M. Nakagawa, "Fundamental analysis for visible-light communication system using LED lights," *IEEE Transactions on Consumer Electronics*, vol. 50, pp. 100–107, Feb. 2004.